Dawn–Dusk Confinement of Magnetic Reconnection Site in the Near-Earth Magnetotail and its Implication for Dipolarization and Substorm Current System

Tsugunobu Nagai[1] and Iku Shinohara[1]

[1]Institute of Space and Astronautical Science, JAXA, Sagamihara, Japan.

Corresponding author: Tsugunobu Nagai (nagai@stp.isas.jaxa.jp)

Key Points:

- The dawn–dusk extent of magnetic reconnection site occupies only the 1-h magnetic local time sector in the near-Earth magnetotail.
- Upward field-aligned currents form in magnetic reconnection site.
- The center of global substorm current system is located just east of the magnetic reconnection site meridian.

Abstract

The dawn–dusk confinement of magnetic reconnection site in the near-Earth magnetotail is established on the basis of Geotail observations. Geotail has made more than 50 encounters with magnetic reconnection in association with the onset of substorms in the near-Earth magnetotail at radial distances of 20–30 R_E in the period of 1994–2019. Ground magnetic field observations are examined for these events, and geosynchronous spacecraft observations are investigated for a limited number of cases. The magnetic reconnection site is located in the upward (from the ionosphere to the tail) field-aligned current part of large-scale substorm current system derived from ground mid-latitude magnetic variations. The site is confined to the localized dawn–dusk extent of the 1-h local time, just west of the center of the large-scale substorm current system. The short dawn-dusk length of the X-line implies that magnetic reconnection inherently proceeds as the two-dimensional dynamics in the magnetotail meridional plane. Rapid dipolarization with upward field-aligned currents occurs at geosynchronous altitude near the meridian of the magnetic reconnection site. This study demonstrates that rapid dipolarization in the inner magnetosphere is produced with earthward outflows from magnetic reconnection and that intense upward field-aligned currents are a direct consequence of magnetic reconnection.

1 Introduction

Magnetic reconnection is a primary engine for the dynamics of magnetospheric substorms. Energy is accumulated in the magnetotail during the growth phase of substorms, and is explosively released via magnetic reconnection during the expansion phase of substorms. Magnetic reconnection initially forms in the near-Earth magnetotail at a downtail distance from -20 R_E to -30 R_E (e.g., Nagai et al., 1998). Fast tailward plasma flows with southward magnetic fields are identified as signatures of magnetic reconnection tailward of the magnetic reconnection site and are frequently observed during substorm activities with spacecraft (e.g., Interplanetary Monitoring Platform IMP–6, IMP–8, Geotail, Cluster, Time History of Events and Macroscale Interactions during Substorms THEMIS, and recently Magnetospheric Multiscale MMS) at radial distances of > 20 R_E (e.g., Hones & Schinder, 1977; Nagai & Machida,1998; Eastwood et al., 2010; Imber et al., 2011; Torbert et al., 2018). However, in situ observations of magnetic reconnection are fairly rare even when spacecraft are at downtail distances from -20 R_E to -30 R_E. Magnetic reconnection proceeds along the X-line, and its width in the tail direction is estimated to be less than a few ion inertial lengths (e.g., Nagai et al., 2011, 2013b). The dawn–dusk length of the X-line has not been unambiguously determined, because there are no in situ observations for magnetic reconnection with two or more separated positions in the dawn–dusk direction of the magnetotail. Nagai et al. (2015b) compiled a survey of magnetic reconnection events observed in the near-Earth magnetotail by Geotail in the period of 1994–2014. Magnetic reconnection can be found in the large dawn–dusk spatial region from Y = +15 R_E to Y = -10 R_E (see also Genestreti et al., 2013, 2014). Magnetic reconnection in the far-dusk and far-dawn sectors of the magnetotail tends to occur during highly disturbed (large Kp) conditions and seems to be associated with a large-scale substorm. It can be imagined that the X-line extends in the dawn–dusk direction. Indeed, Nakamura et al. (2012) suggested the dawnward development of the magnetic reconnection site in Hall magnetohydrodynamic (MHD) simulations (see also Huba & Rudakov, 2002; Shay et al., 2003). However, a long dawn–dusk length of the X-line appears to be inconsistent with the rare encounters of the magnetic reconnection site in spacecraft observations.

In 2015–2019, the National Oceanic and Atmospheric Administration Geostationary Operational Environmental Satellites GOES made continuous energetic proton and electron observations with high time resolution magnetic field measurements at multiple positions at 6.6 R_E (see Nagai et al., 2019). A large number of digital ground magnetic field data then became available. Fortunately, Geotail returned to the plasma sheet in 2015–2017 after a long stay in the tail lobes in its tail seasons and was able to provide in situ observations of magnetic reconnection. We investigate the relationship between the magnetic reconnection site and the substorm current system inferred from the ground magnetic field observations. A substorm current system can be modeled using the concept of a substorm current wedge proposed by McPherron et al. (1973). A current wedge is composed of downward (into the ionosphere) field-aligned currents in the eastern part and upward (from the ionosphere) field-aligned currents in the western part. These field-aligned currents produce a positive bay signature in the northward component, H, of the magnetic field at mid- and low-latitudes on the ground. The effect of these field-aligned currents is observed as changes in the east-west component, D, of the magnetic field at mid-latitudes on the ground and in the vicinity of the geosynchronous altitude in space. The eastern downward field-aligned currents produce negative D variations (the western deflection) and the western upward field-aligned currents produce positive D variations (the eastward deflection) in the Northern Hemisphere (e.g., Nagai, 1982, 1987). The D sign is opposite in the Southern Hemisphere. A simple line current model with the dawn–dusk symmetric structure is given by Nagai (1987), and the center of the current wedge can be estimated at the meridian of zero D deflection, where the positive H bay has its peak amplitude. However, it is known that a real substorm current system shows strong dawn–dusk asymmetry (e.g., Baumjohann et al., 1981). The western upward field-aligned currents are intense and highly localized and are likely connected with active aurorae, such as the westward traveling surge. The eastern downward field-aligned currents are less intense but are widely distributed in the morning sector. There are events in which the longitudinal range of the negative D deflection is wider than that of the positive D deflection (e.g., Clauer and McPherron, 1974). However, the zero D deflection meridian is used as the center of the substorm current system in this paper for simplicity.

This study presents the somewhat unexpected result that magnetic reconnection in the near-Earth magnetotail is observed only in the upward field-aligned current region. Magnetic reconnection in the far-dusk (+Y) and far-dawn (−Y) sectors of the magnetotail is associated with a newly formed substorm current wedge in these regions. Furthermore, rapid dipolarization at geosynchronous altitude occurs only near the magnetic reconnection meridian. These results are verified with statistical studies with more than 50 events. The statistical studies clearly demonstrate the dawn–dusk confinement of the magnetic reconnection site in the near-Earth magnetotail.

In this paper, Section 2 describes the data used in this study. Section 3 describes three clear-cut events showing the relationship between the magnetic reconnection site and the substorm current system and dipolarization at geosynchronous altitude. Section 4 describes the statistical studies. Section 5 discusses the significance of the present results with respect to the substorm dynamics. The conclusions are given in Section 6. Signatures of in situ magnetic reconnection in the magnetic field and plasma observations with Geotail have already been described in detail in previous studies (Nagai et al., 1998, 2001, 2011, 2013a, 2013b, 2015a,

2015b) with a review given by Nagai (2021), and are known to be common in spacecraft observations, e.g., Cluster, THEMIS, and MMS (Nakamura et al., 2006; Oka et al., 2016: Torbert et al., 2018); therefore, we only present the key signatures for the magnetic reconnection events in this paper. The most essential signature is strong electron acceleration/heating during high-speed plasma flows. Various expected Hall physics of magnetic reconnection can be found with electron acceleration/heating, as discussed in detail in, e.g., Nagai et al. (2011, 2013b). Hence, the magnetic reconnection site, which is also called the X-line in appropriate cases, is defined as the region where electrons show acceleration/heating.

2 Data

In situ magnetic reconnection observations were made with the spacecraft Geotail. The magnetic field data were obtained with the magnetic field experiment MGF (Kokubun et al.,1994), and the ion and electron data were obtained with the low-energy plasma experiment LEP (Mukai et al., 1994). Full energy-time spectrograms for the ions and electrons from LEP, which are the most fundamental data used to identify magnetic reconnection, are given on the Institute of Space and Astronautical Science (ISAS) website, and can be obtained on the CDAWeb site. The Geotail data are given using the geocentric solar magnetospheric (GSM) coordinate system. For the event studies during the period of 2015–2017, we used data obtained by GOES-13 at 75° W, GOES-14 at 105° W, and GOES-15 at 135° W. Magnetic field data with a time resolution of 0.512 s are given using in the VDH coordinate system. In the VDH system, H (pointing northward) is antiparallel to the Earth's dipole axis, D (azimuthal east) is orthogonal to H and a radius vector to the satellite, and V (nearly radial outward) completes the Cartesian coordinate system. Therefore, the directions of the H and D components are the same as those used for the ground magnetic field data. The Energetic Particle Sensor MAGnetospheric Proton Detector provides proton (>80 keV) fluxes in five channels and the Energetic Particle Sensor MAGnetospheric Electron Detector provides electron (>30 keV) fluxes in five channels; more detailed information is available in Nagai et al. (2019). In addition, we use 1-min average magnetic field data from other GOES spacecraft. The ground magnetic field data consist of 1-s digital data (from Kakioka and US stations) and 1-min digital data (from other stations). However, some data from the US stations (mostly prior to 2010) are 1-min digital data. In this study, the magnetic field data are presented using the H (northward) component and D (eastward) component. Even when the digital data are given as X- and Y-component data, these data are used as H- and D-component data. The data used in this study are from mid- and low-latitude stations; therefore, there is no significant discrepancy between these two coordinate systems. The station name and ABB (abbreviation) code are used according to the World Data Center for Geomagnetism, Kyoto, Data Catalogue, No. 32. The information for the geographic and geomagnetic locations of the ground stations are presented in the Data Catalogue. In this study, the Geotail footpoint is determined via SSCWEB and all local magnetic time values are calculated using GEOPAC.

3 Event studies

We first examine the events on 16 September 2017 (Section 3.1). Two substorms successively occurred when Geotail was in the dusk magnetotail where magnetic reconnection is most frequently observed. Geotail made in situ observation of magnetic reconnection for the second substorm; however, no reconnection signatures were detected for the first substorm. The ground magnetic field observations clearly show a difference in the central meridians of the

substorm current systems for these two events. Rapid dipolarization occurred only near the meridian of the magnetic reconnection site at geosynchronous altitude. Second, we examine the events on 4 October 2015. At this time, Geotail was located in the far-dusk sector of the magnetotail (Y_{GSM} = +18 R_E) and made in situ observation of magnetic reconnection. The ground magnetic field data demonstrate the formation of the substorm current system on the far-dusk side. Third, we examine the events on 4 October 2016, in which Geotail observed magnetic reconnection in the far-dawn sector of the magnetotail (Y_{GSM} = −10 R_E). Rapid dipolarization at geosynchronous altitude proceeded at an unusually late magnetic local time (MLT) location (04 MLT). The substorm current system newly formed on the far-dawn side. These three events clearly demonstrate that upward field-aligned currents flow in the field lines connected with magnetic reconnection which proceeds in any MLT range.

3.1 The 16 September 2017 event

Figure 1 shows the ground magnetic field variations for the period from 0400 UT to 0600 UT on 16 September 2017. The H and D data from six US stations (the most western station being Fresno FRN and the most eastern station being San Juan SJG) covering the 20–01 MLT range are presented. There were two major substorm onsets near 0430 UT and 0500 UT identified by positive bay onsets in H, even though the second substorm had multiple onset signatures. The AL index exceeded −800 nT for the first substorm and −1000 nT (only a short duration) for the second substorm, while the magnitude of the positive bay in H was nearly the same for both events. A major difference was observed with respect of the central meridian of the substorm current system. The central meridian for the first substorm was located between Boulder (BOU; +D deflection at 21:11 MLT) and Stennis (BSL; −D deflection at 22:27 MLT), while the central meridian for the second substorm was located near FRD (small positive D at 23:52 MLT). Note that the D defection was negative for the first substorm and positive for the second substorm at BSL close to the meridian of the Geotail field line footpoint (approximately 22:30 MLT).

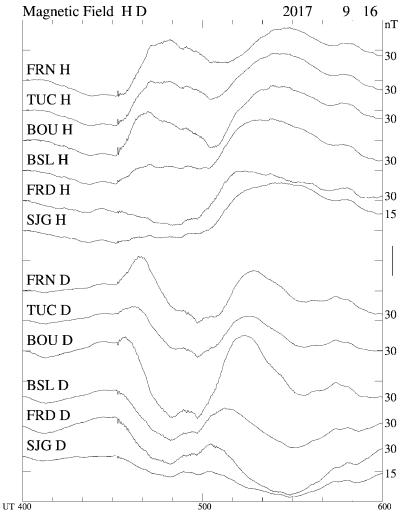

Figure 1. Ground magnetic field data (H and D components) from Fresno (FRN), Tucson (TUC), Boulder (BOU), Stennis (BSL), Fredericksburg (FRD) and San Juan (SJG) for the period of 0400–0600 UT on 16 September 2017. The vertical line on the right side corresponds to 30 nT for FRN, TUC, BOU, BSL, and FRD and 15 nT for SJG.

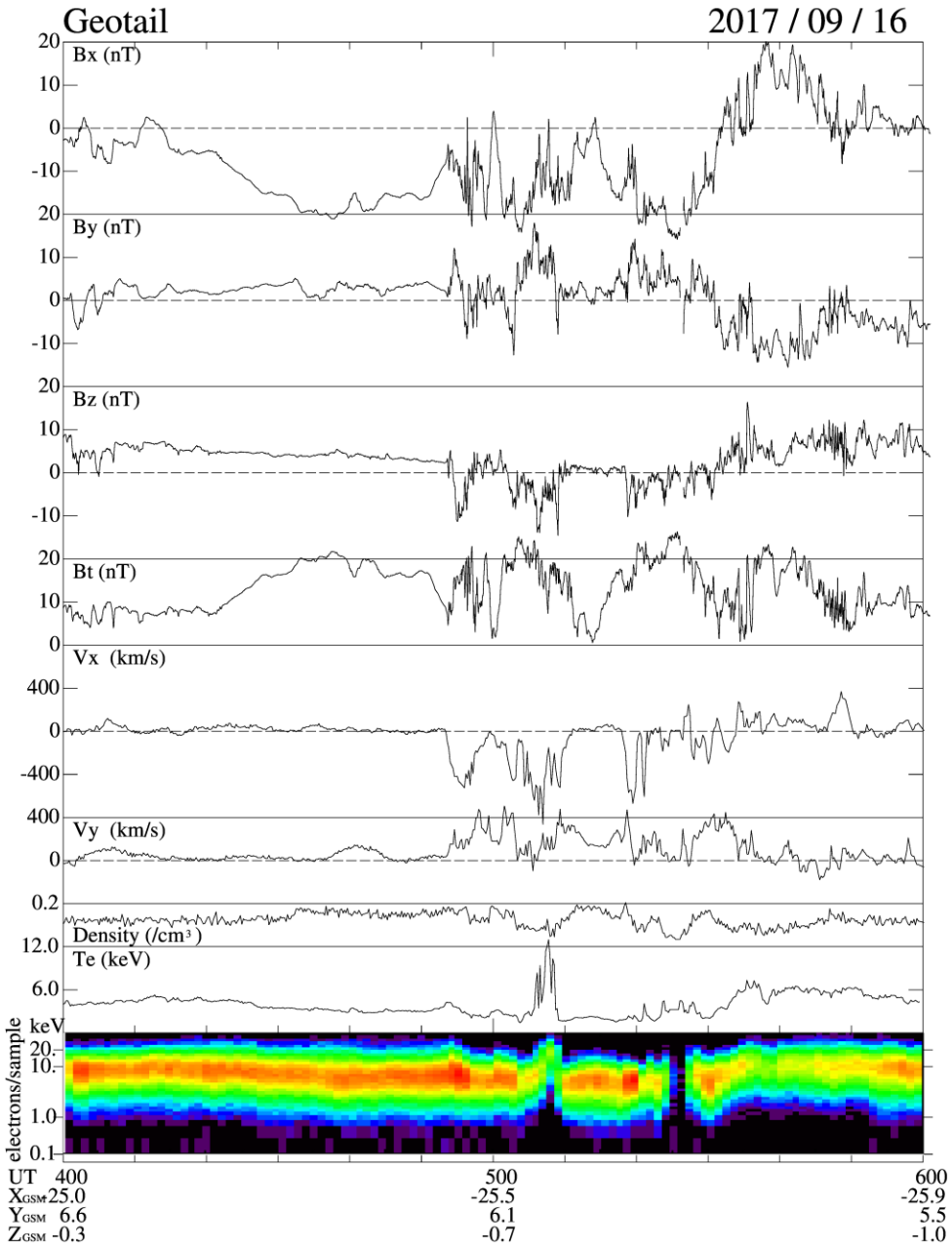

Figure 2. Magnetic reconnection observations by the spacecraft Geotail for the period of 0400–0600 UT on 16 September 2017. From top to bottom: magnetic field Bx, By, Bz, and Btotal (Bt) [nT], ion flow velocity Vx and Vy [km s^{-1}], number density [cm^{-3}], electron temperature [keV] and electron energy-time spectrogram. Electron counts are presented with a color code (red for high flux and blue for low flux) in the energy (0.1–40 keV)-time spectrogram.

Figure 2 shows the magnetic field and plasma observations made by Geotail at X_{GSM} = −25.5 R_E, Y_{GSM} = +6.1 R_E, and Z_{GSM} = −0.7 R_E at 0500 UT. For the second substorm, Geotail observed fast tailward flows with negative Bz starting at 0452 UT. The flow velocity Vx became nearly zero at 0500 UT, and new activity started after 0500 UT. An intense electron acceleration occurred after 0505 UT, as identified by the disappearance of low-energy (< 1 keV) electrons in the electron energy-time spectrogram. This is the most important key signature for magnetic reconnection (e.g., Nagai, 2021). Simultaneously, the electron temperature rose to more than 10 keV and the electron flow velocity Vx exceeded −3500 km s^{-1} (not shown) when the ion flow velocity was −800 km s^{-1}. The magnetic field By then became significantly positive in the Southern Hemisphere (Bx < 0). These changes indicate ion-electron decoupling (Hall physics) in the magnetic reconnection site. Conversely, no substorm onset signatures were observed inside the plasma sheet for the 0430 UT onset substorm. Indeed, the plasma density slightly increased, the plasma temperature slightly decreased, and there was no flow activity. Coupled with the increase in the total magnetic field Bt, these are typical signatures of the substorm growth phase in the plasma sheet (e.g., Nagai et al., 1997; Shukhtina et al., 2014).

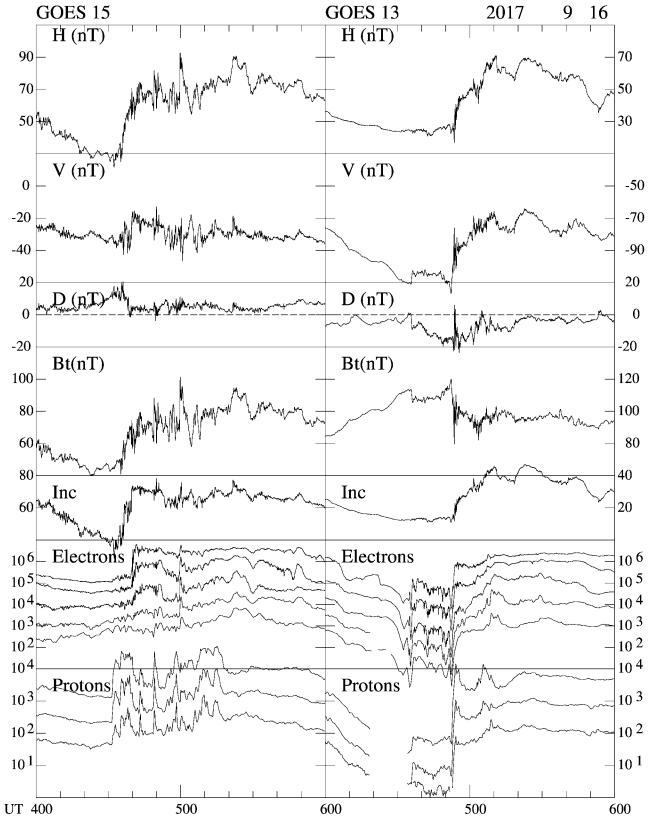

Figure 3. The magnetic field (H, V, D, and Btotal in nT and inclination in degrees) and the 30–50-, 50–100-, 100–200-, 200–350-, and 350–600-keV electron and 80–110-, 110–170-, 170–250-keV proton fluxes for GOES-15 and GOES-13 for the period of 0400–0600 UT on 16 September 2017. The electron and proton fluxes are given in $cm^{-2}\ s^{-1}\ sr^{-1}\ keV^{-1}$.

Figure 3 shows the particle and magnetic field behaviors observed by GOES-15 at 135° W and GOES-13 at 75° W. For the second substorm, intense dipolarization was observed only by the eastern spacecraft GOES-13 (at 00:00 MLT). The electron fluxes showed increases, likely recovery to the pre-substorm level in association with the dipolarization in the magnetic field. The proton fluxes showed enhancement. There was an intense positive D spike during the dipolarization, indicating the occurrence of proton injection. Proton injections are always accompanied by a positive D perturbation indicating the flow of upward field-aligned currents (Nagai et al., 2019). Furthermore, GOES-15 (at 4 h earlier MLT) observed energy-dispersive drifting protons for the second substorm. These signatures indicate that intense dipolarization took place near the GOES-13 median; this is consistent with the ground magnetic field observations. For the first substorm at 0430 UT, dipolarization and proton injections were only observed by GOES-15 (at 19:33 MLT).

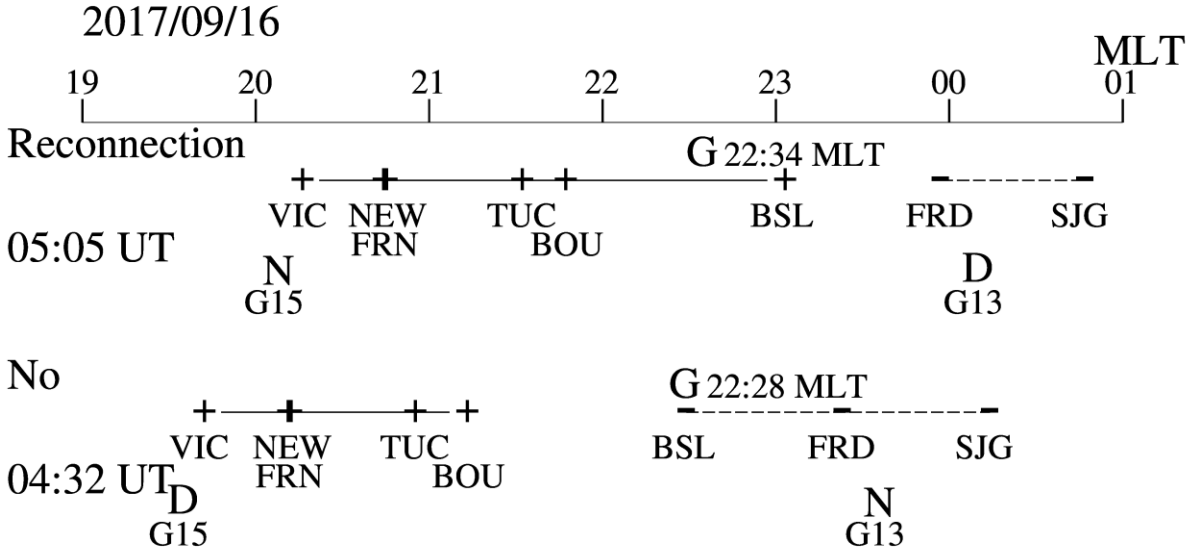

Figure 4. Summary of the 0505 UT and 0432 UT events on 16 September 2017. The Geotail magnetic local time (MLT) location (represented by G) is shown at 22:34 MLT for the 0505 UT event and at 22:28 MLT for the 0432 UT event. The D deflection at the ground station is indicated by "+" for positive and "-" for negative at its MLT position. The positive D deflection region corresponding to the upward field-aligned current region is indicated by a horizontal line, while the negative D deflection region corresponding to the downward field-aligned current region is indicated by a dashed horizontal line. The rapid dipolarization at geosynchronous altitude is indicated by D with G13 indicating GOES-13 and with G15 indicating GOES-15. N indicates less pronounced dipolarization.

These observations are summarized in Figure 4. For the second substorm near 0500 UT, magnetic reconnection proceeded at Geotail in the 22:34 MLT meridian, just west of BSL (at 23:03 MLT), where the D deflection was positive, such that Geotail was located in the upward field-aligned current region. For the first substorm at 0430 UT, Geotail was located at the 22:28 MLT meridian, where the negative D deflection was observed at the same meridian on the ground (BSL was located at 22:27 MLT). Therefore, Geotail was in the downward field-aligned current region.

3.2 The 4 October 2015 event

An intense substorm (with a minimum AL of -1500 nT) started near 0600 UT on 4 October 2015 under highly active conditions. As can be seen in Figure 5, a positive bay was recorded in the Pacific area, indicating that the substorm activity occurred on the far-dusk side. Honolulu (HON; at 19:25 MLT) showed a positive D deflection, while Fresno (FRN; at 21:48 MLT) showed a negative D deflection. The central meridian of the substorm current system was likely near Papeete (PPT; at 20:26 MLT).

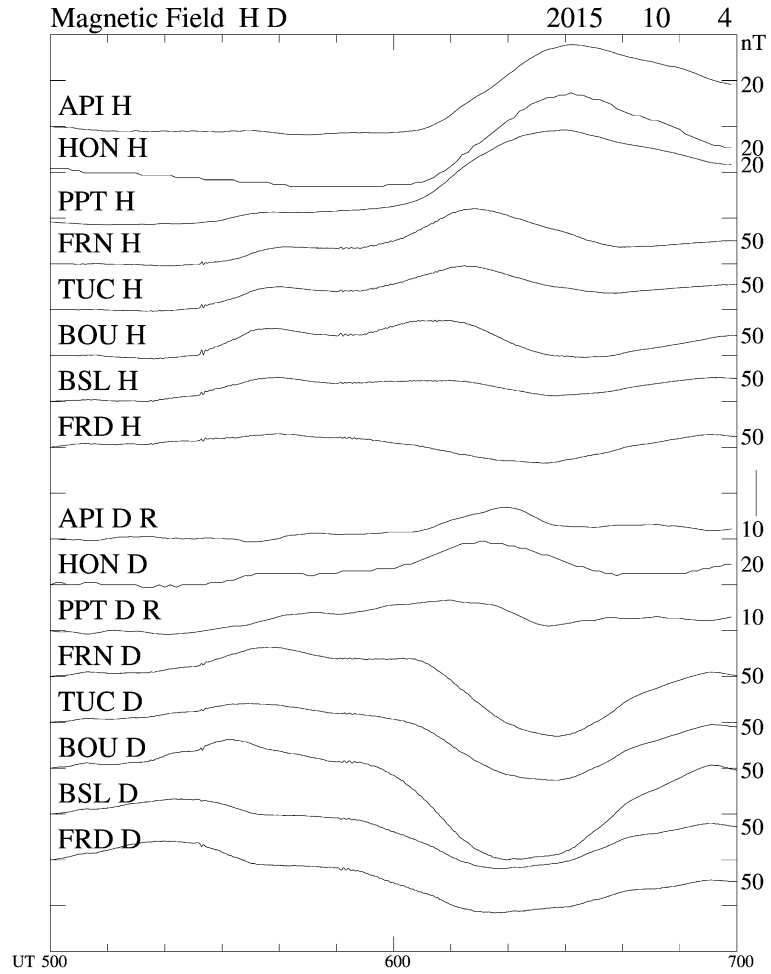

Figure 5. Ground magnetic field data (H and D) from Apia (API), Honolulu (HON), Papeete (PPT), Fresno (FRN), Tucson (TUC), Boulder (BOU), Stennis (BSL), and Fredericksburg (FRD) for the period of 0500–0700 UT on 4 October 2015. The sign of the D component from the Southern Hemisphere stations API and PPT is reversed. The vertical line on the right side corresponds to 20 nT for API, PPT, and HON and 50 nT for the other stations. For D, the vertical line on the right side corresponds to 10 nT for API and PPT.

Geotail stayed at $X_{GSM} = -23.6\ R_E$, $Y_{GSM} = +18.4\ R_E$, and $Z_{GSM} = -0.5\ R_E$ for this substorm and observed signatures of magnetic reconnection, as shown in Figure 6. There were a

number of flow reversals with the Bz reversals, as well as simultaneous detections of electron acceleration. GOES-15 (at 21:11 MLT) observed dipolarization and proton injections at 0550 UT, as shown in Figure 7, in an earlier MLT region in comparison to usual events (Nagai et al., 2019). The D deflection at GOES-15 was positive and an intense positive D spike is associated with the second proton injection, even though no or a negative deflection was observed in D at FRN on the ground (Figure 5).

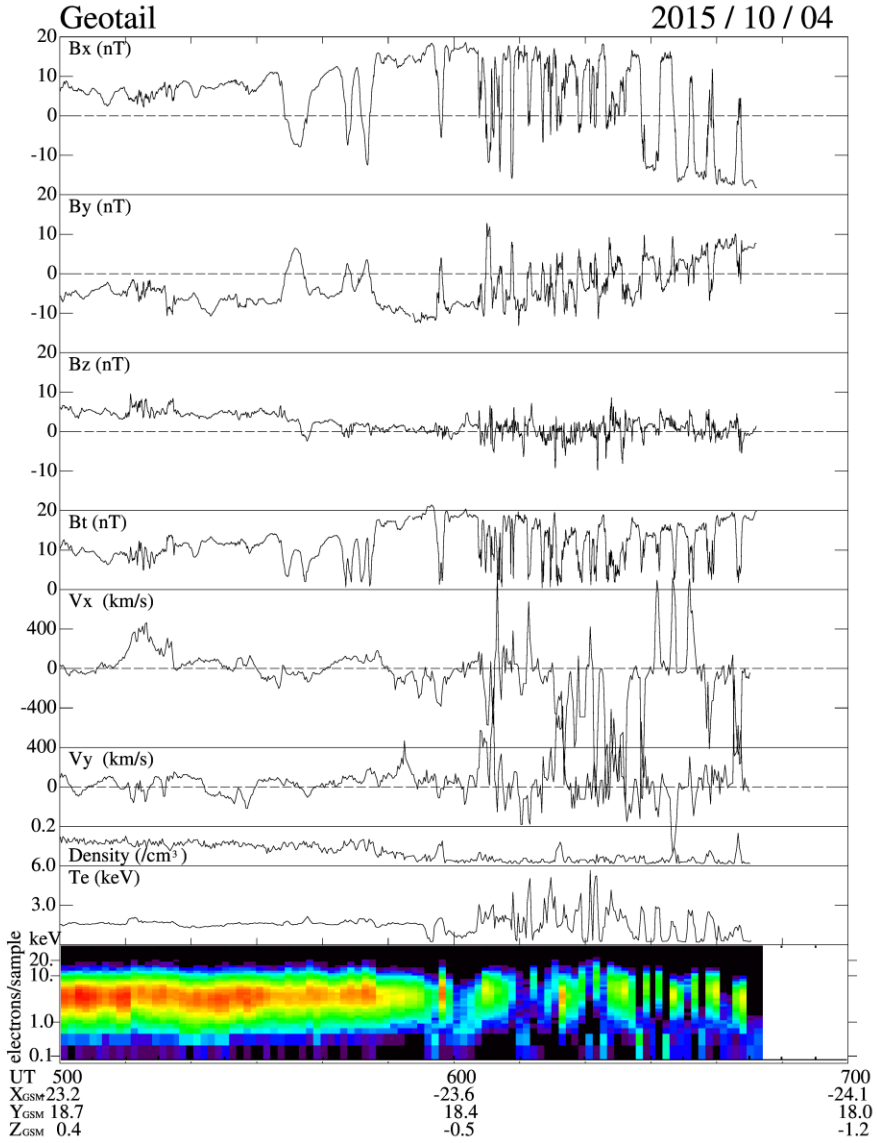

Figure 6. Magnetic reconnection observations by the spacecraft Geotail for the period of 0500–0700 UT on 4 October 2015. From top to bottom: magnetic field Bx, By, Bz, and Btotal [nT], ion flow velocity Vx and Vy [km s^{-1}], number density [cm^{-3}], electron temperature [keV] and electron energy-time spectrogram.

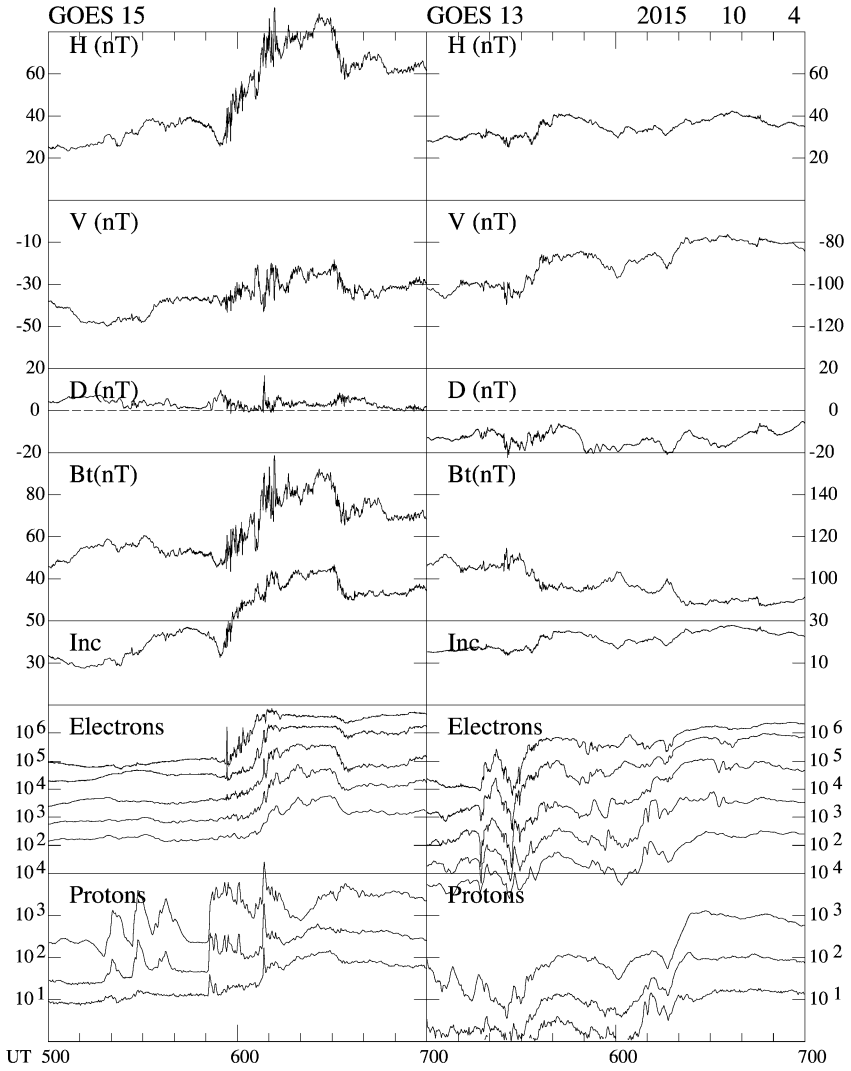

Figure 7. The magnetic field (H, V, D, and Bt in nT and inclination in degrees) and the 30–50-, 50–100-, 100–200-, 200–350-, and 350–600-keV electron and the 80–110-, 110–170-, 170–250-keV proton fluxes for GOES-15 and GOES-13 for the period of 0500–0700 UT on 4 October 2015. The electron and proton fluxes are given in $cm^{-2}\ s^{-1}\ sr^{-1}\ keV^{-1}$.

These observations are summarized in Figure 8. Because the Geotail footpoint was located at the 19:43 MLT meridian (near the HON meridian), Geotail was in the upward field-aligned current region. There was another substorm that started at 0525 UT on 4 October 2015, and the center of this substorm current system was located between BOU (at 22:14 MLT) and BSL (at 23:30 MLT). The MLT location of the substorm center was not extraordinary, and the AL index exceeded -500 nT. Geotail did not detect any substorm signatures for this substorm, even though Geotail was in the upward field-aligned current region.

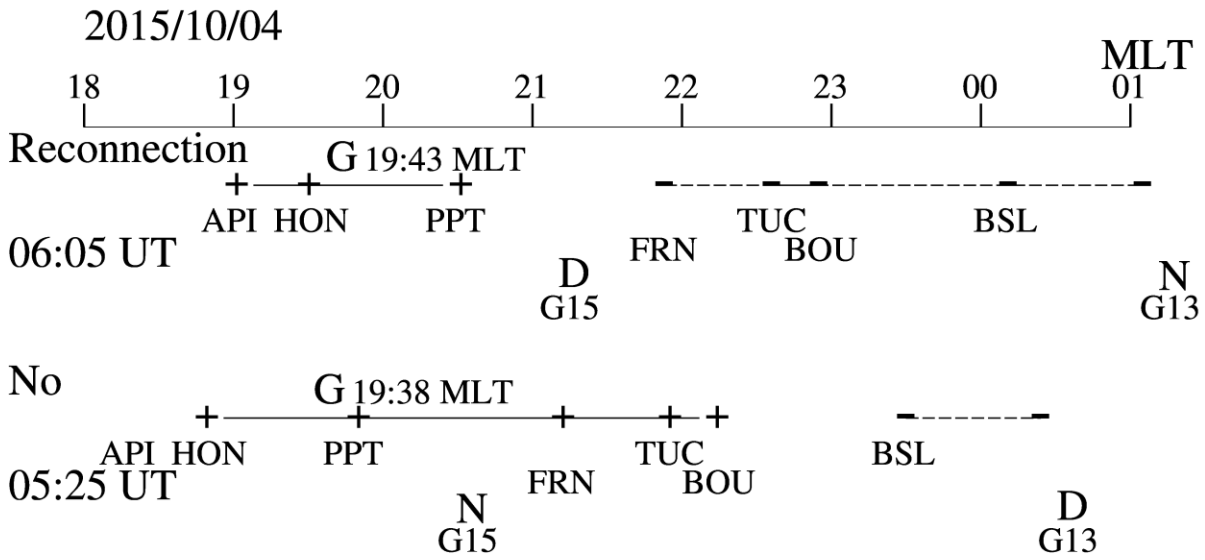

Figure 8. Summary of the 0605 UT and 0525 UT events on 4 October 2015, notation as in Figure 4.

3.3 The 4 October 2016 event

Intense substorm activity occurred on 4 October 2016, and there were two clear positive bays starting at 1150 UT and 1250 UT. Selected ground magnetic field data are presented in Figure 9. D-component data from HON are not available. The D variations at Apia (API; west of HON) and at Papetee (PPT; east of HON) were nearly the same. The central meridian of the substorm current system was located near Charters Towers (CTA; at 21:59 MLT) for the 1150 UT onset substorm. For the 1250 UT onset substorm, the central meridian was located between PPT (at 03:15 MLT) and FRN (at 04:38 MLT), unusually in the late morning sector.

Figure 10 shows the magnetic field and plasma observations made by Geotail. Geotail observed electron heating at 1257 UT for the second substorm at $X_{GSM} = -23.4\ R_E$, $Y_{GSM} = -9.9\ R_E$ and $Z_{GSM} = -1.8\ R_E$. The Geotail footpoint was located at 01:34 MLT. Note that this observation was made near the neutral sheet deep inside the plasma sheet, because Bx made the zero crossing. Therefore, the accelerated electrons were not streaming near the tail lobe/plasma sheet boundary. Indeed, the electron bulk velocity Vx exceeded -3000 km s^{-1} (not shown) when the ion bulk velocity Vx was -800 km s^{-1}. Geotail only observed MHD tailward flows for the first substorm, and no in situ magnetic reconnection signatures were observed.

Figure 11 shows magnetic field and particle observations from GOES-15 at 135° W and GOES-14 at 105° W. At 1257 UT, a sharp dipolarization with a negative D deflection took place at GOES-15, which was located at 04:08 MLT. Variations at geosynchronous altitude are usually gradual in this local time sector. There were nearly no changes at GOES-14 at 06:07 MLT. For the first substorm starting at 1150 UT, GOES-15 and GOES-14 observed drifting (energy-dispersive) protons and electrons and there were no significant changes in the magnetic field.

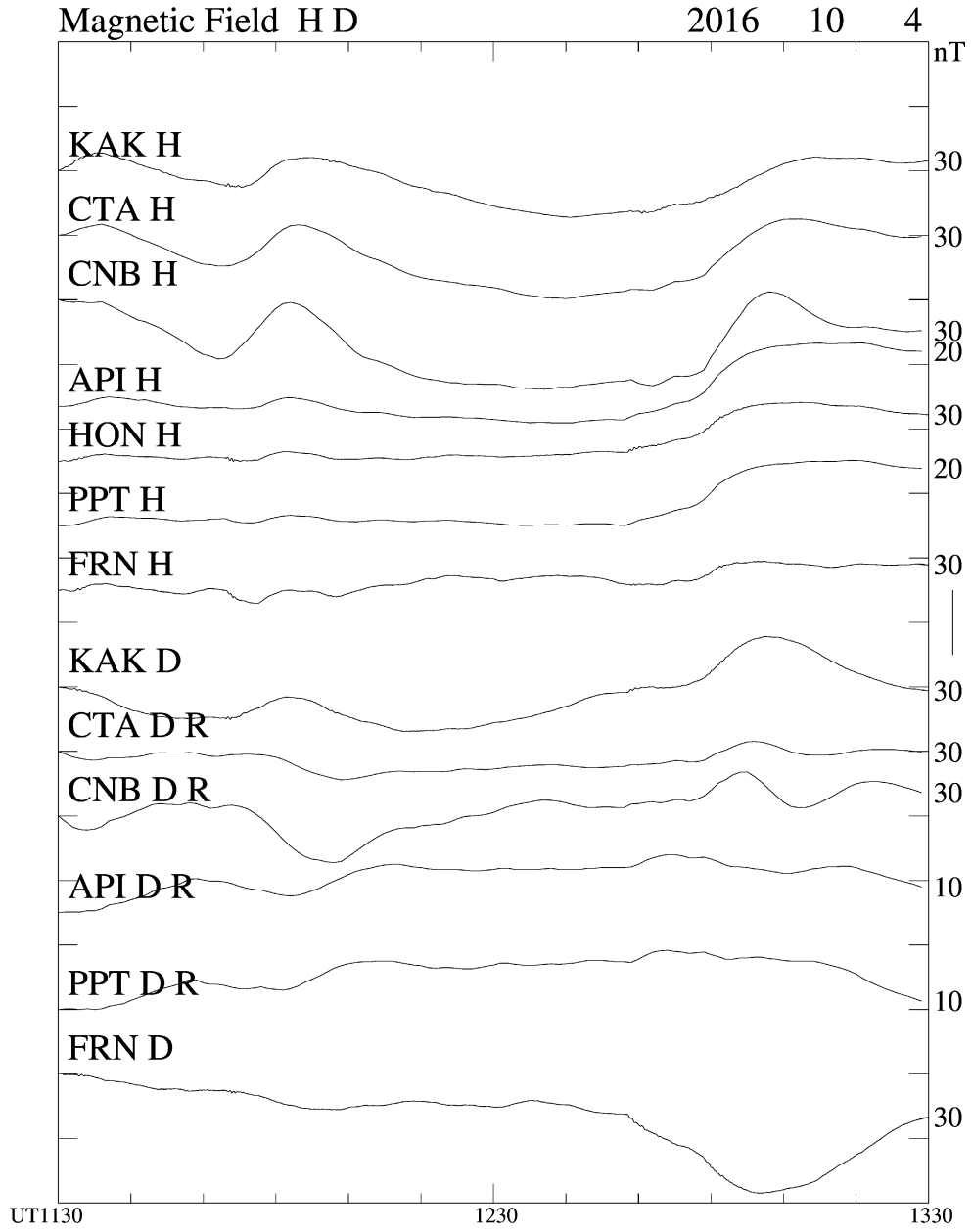

Figure 9. Ground magnetic field data (H and D) from Kakioka (KAK), Charters Towers (CTA), Canberra (CNB), Apia (API), Honolulu (HON), Papeete (PPT), and Fresno (FRN) for the period of 1130–1330 UT on 4 October 2016. The sign of the D component from the Southern Hemisphere stations CTA, CNB, API, and PPT is reversed. The vertical line on the right side corresponds to 20 nT for API, HON, and PPT and 30 nT for the other stations. For D, the vertical line on the right side corresponds to 10 nT for API and PPT.

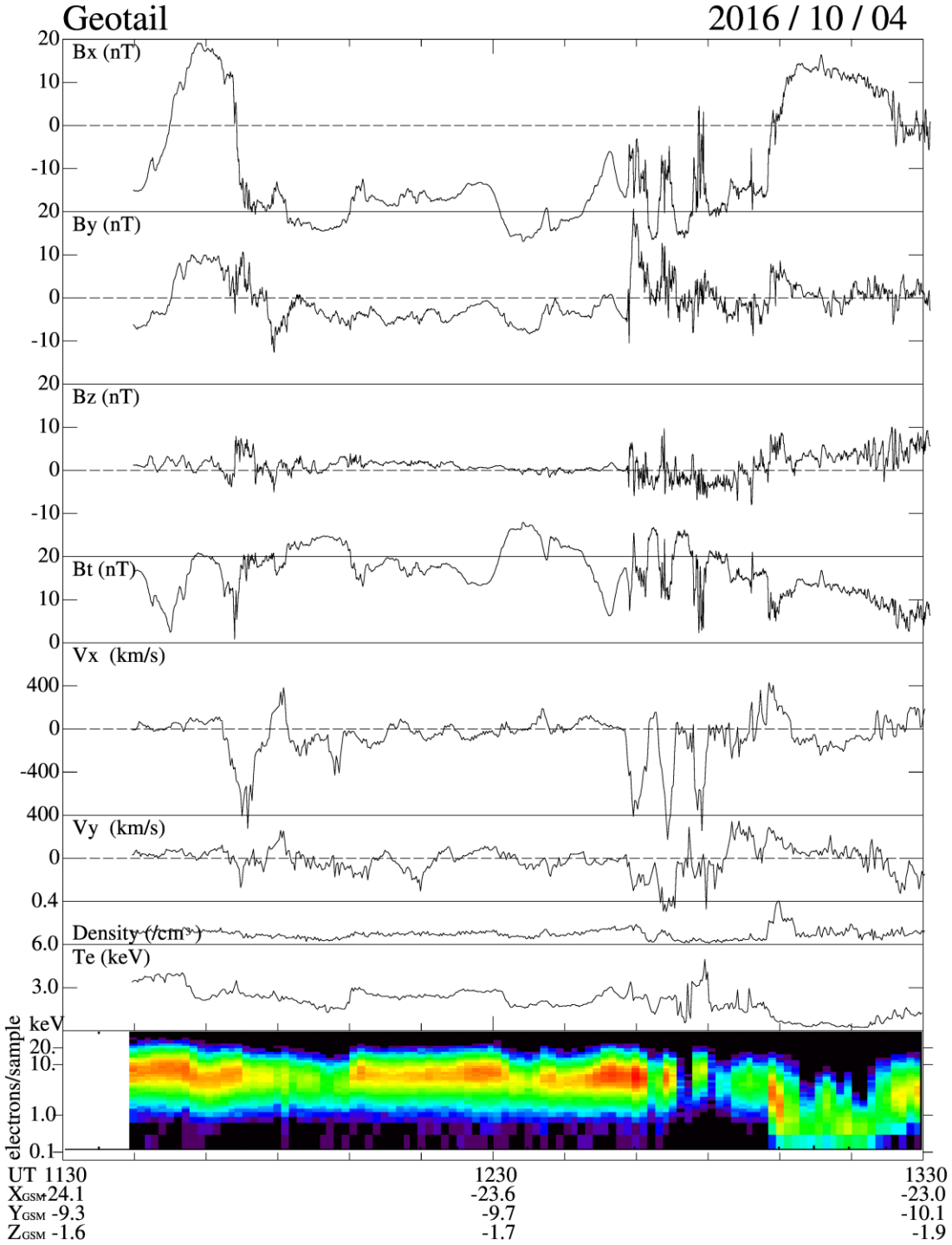

Figure 10. Magnetic reconnection observations by Geotail for the period of 1130–1330 UT on 4 October 2016. From top to bottom: magnetic field Bx, By, Bz, and Btotal [nT], ion flow velocity Vx and Vy [km s^{-1}], number density [cm^{-3}], electron temperature [keV] and electron energy-time spectrogram.

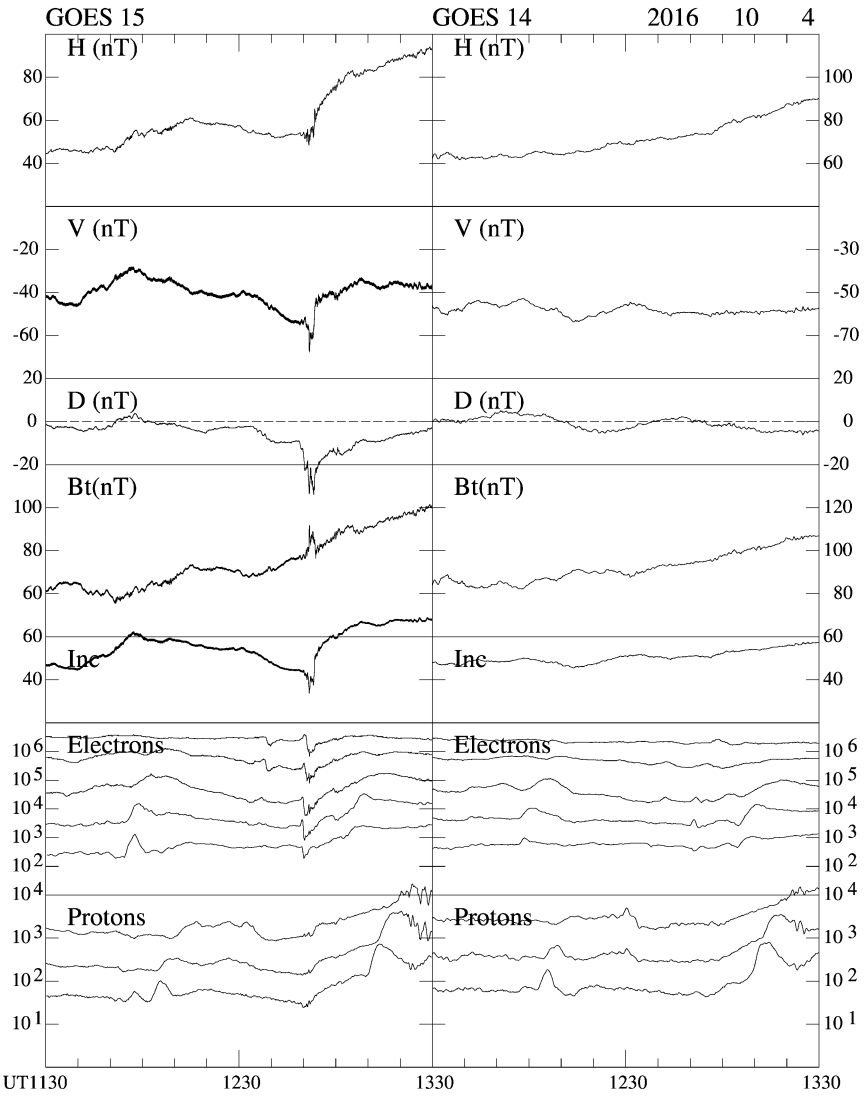

Figure 11. The magnetic field (H, V, D, and Bt in nT and inclination in degrees), the 30–50-, 50–100-, 100–200-, 200–350-, and 350–600-keV electron and, the 80–110-, 110–170-, 170–250-keV proton fluxes for GOES-15 and GOES-13 for the period of 0400–0600 UT on 4 October 2016. The electron and proton fluxes are given in $cm^{-2}\ s^{-1}\ sr^{-1}\ keV^{-1}$.

Figure 12 summarizes the observations for the 4 October 2016 events. During the second substorm starting at 1250 UT, Geotail observed in situ magnetic reconnection even in the far-dawn sector of the magnetotail at $Y_{GSM} = -10\ R_E$ (at 01:34 MLT). For this substorm, the center of the substorm current system formed near the 04:00 MLT meridian and rapid dipolarization occurred even in the late morning sector at 04:08 MLT. Geotail was located in the upward field-aligned current region during this substorm. Conversely, the first substorm starting at 1152 UT did not show any unusual characteristics. The center of the substorm current system was located

near the 22:00 MLT meridian, and almost no onset signatures were observed in the dawn sector at geosynchronous altitude and in the magnetotail.

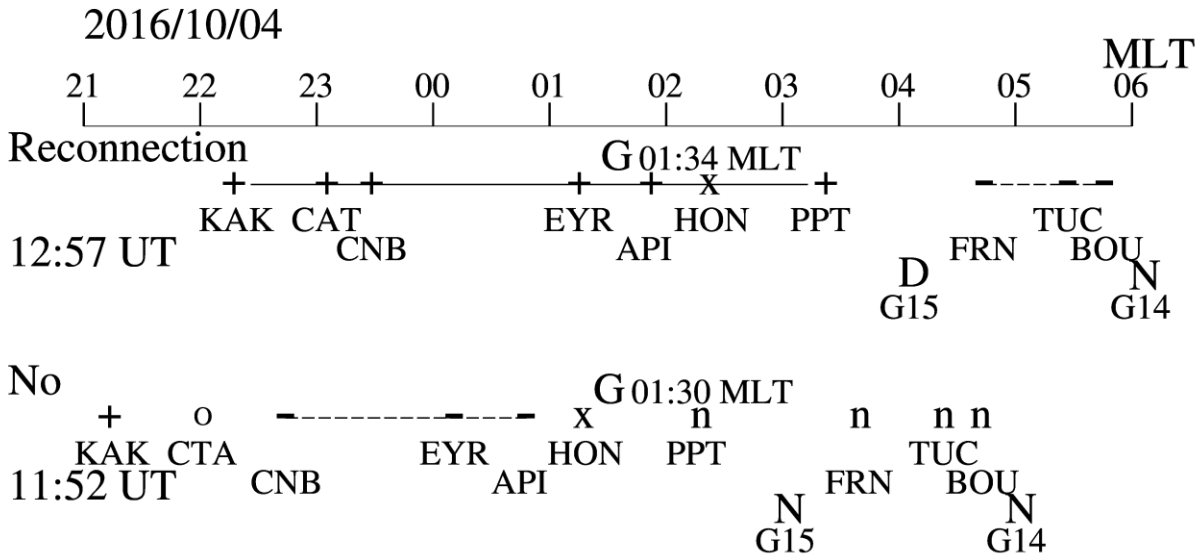

Figure 12. Summary of the 1257 UT and 1152 UT events on 4 October 2016, notation as in Figure 4.

4 Statistical studies

We conducted statistical studies to confirm the important findings in the event studies described in Section 3 and to identify general characteristics of magnetic reconnection and its related dynamics. We obtained 71 magnetic reconnection events from the 1994–2014 survey in the magnetotail, $X_{GSM} < -20\ R_E$, with the primary selection criterion being electron acceleration/heating during fast plasma flows (Nagai et al., 2015b). Using the same procedure, we obtained 11 magnetic reconnection events in 2015–2017. We did not find observations of any in situ magnetic reconnection events satisfying the adopted criteria in the period of 2018–2019, primarily because Geotail was usually in the tail lobe in the tail season during these years. To determine the central meridian of a substorm current system, we require digital ground magnetic field data at mid-latitudes from several stations for each event. Furthermore, we need to unambiguously identify a positive bay signature. The adopted criterion was that the amplitude of the positive bay exceeds 10 nT at least at one station for each event. Using this criterion, we obtained 56 events (45 events in 1994–2014 and 11 events in 2015–2017). On average, there were five stations for each event (including two stations with positive D variation and two stations with negative D variation). In these 56 events, flow reversals (for example, the 04 October 2015event in Section 3.2) are observed for 42 events. Only tailward flows with electron acceleration/heating (for example, the 16 September 2017 event in Section 3.1) are observed for 14 events, including the events in which Geotail entered the tail lobe. These are no differences in their characteristics between these two classes, as described by Nagai et al. (2015b). Figure 13 shows the Geotail footpoint locations in the MLT versus the geomagnetic latitude diagram and the GSM positions in the magnetotail x-y plane. The three events described in Section 3 are indicated in the figure. The event distribution in Figure 13 does not differ significantly from that

for the 71 events in the period of 1994–2014 (Figure 2 in Nagai et al., 2015b); therefore, no bias associated with availability of ground magnetic field data was found. The GOES magnetic field data can be examined for 18 events, because the GOES spacecraft need to be in the pre-midnight sector to identify variations in the magnetic field.

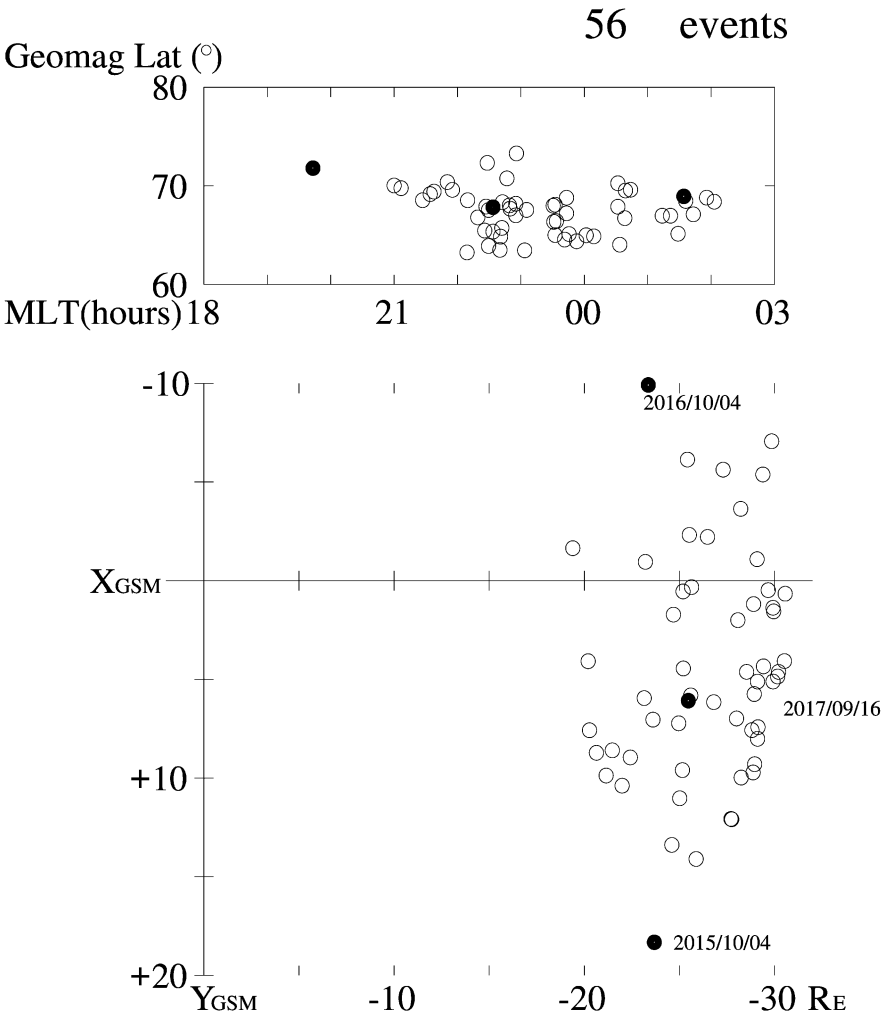

Figure 13. Location of magnetic reconnection events in the Geotail footpoint MLT versus the geomagnetic latitude diagram (upper panel) and in the GSM x-y plane (lower panel). The three dots indicate the events described in Section 3.

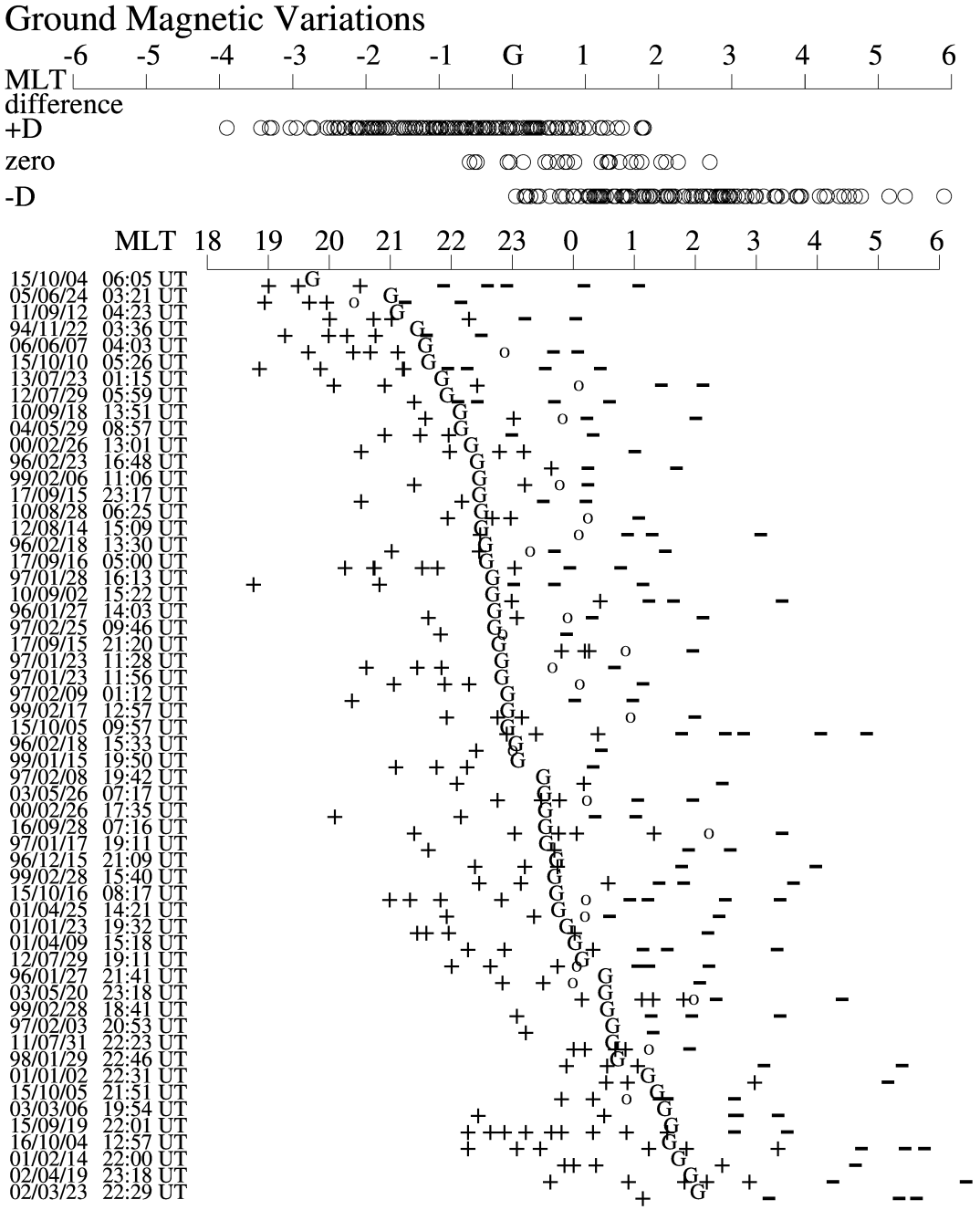

Figure 14. Ground D variations during magnetic reconnection relative to the Geotail footpoint in the MLT diagram. The upper panel shows all the data points (three different classes) from the 56 events, and the lower panel shows the D variations for each event ("+" for positive D, "– " for negative D, and "o" for no variation).

4.1 Ground D variations

Figure 14 shows the D deflection signs near the Geotail footpoint meridian for each event (lower panel). The Geotail meridian spans from 20 MLT to 02 MLT, and many events are found in the 22–24 MLT sector. For these 56 magnetic reconnection events, a reasonable amount of ground station data can be examined. Here, positive D deflections are denoted "+" and the negative D deflections are denoted "−". Cases in which there is nearly no deflection in D for the positive H bay are denoted "o". The D deflection is determined by the sign for the initial 10-min time interval of the positive bay because Geotail almost always observed the magnetic reconnection signatures during this time interval. The positive sign is given when the average D value is > +1.0 nT, while the negative D sign is given when the average D value is < −1.0 nT. When we adopt a 5-min time interval or a criterion of 2 nT, the general characteristics do not change significantly and the number of stations with zero D deflection increase. Following the computer calculations of these values, all data were plotted for visual inspection and no significant errors in the procedure were found. For the low-latitude stations PPT (−15.11° geomagnetic latitude) and API (−15.02° geomagnetic latitude), a D deflection of less than 1.0 nT was adopted because these two stations are important for determining the D variations in the Pacific sector. The upper panel of Figure 14 summarizes the three different classes of D behavior (positive, zero, and negative) relative to the Geotail footpoint meridian.

Geotail is always located in the +D or zero D variation region. There are some events in which negative D variations are observed just east of the Geotail footpoint meridian. For example, at 2151 UT on 5 October 2015 (the 50th 15/10/05 2151 UT event in the lower panel of Figure 14), the D variation was negative at Moscow (MOS; at 01:25 MLT) and Borok (BOX; at 01:33 MLT) and nearly zero at Kiev (KIV; at 00:53 MLT) when the Geotail footpoint was located at 01:22 MLT. Unfortunately, Geotail magnetic field observations were not made because the MGF instrument was stopped as a result of the eclipse (Geotail entered the Earth's shadow). The onboard data processing of the plasma measurements from LEP was incomplete (probably caused by the eclipse), and only several data points from LEP are available. There is a possibility that accelerated electrons were streaming near the plasma sheet boundary; however, we could not examine the event itself in detail. Because the electron acceleration/heating was evident, this event was selected for the present statistics. In the other cases in which negative D deflections were observed just east of the Geotail footpoint meridian, there was a station in which a positive D deflection was observed just west of that meridian.

The center of the substorm current system can be estimated if we allow for some ambiguity. One method is to place the center of the substorm current system in between a station with a positive D deflection and one with a negative D deflection. This method can be adopted for 56 events. The other method is to place the center of the substorm current system at the station with zero D deflection. This method can be used for 24 events. Because we use a variety of geomagnetic latitude stations, it is impossible to quantitively evaluate the amplitude of the D deflection. The magnetic reconnection site relative to the center of the substorm current system is given in MLT in Figure 15. It is evident that magnetic reconnection is most frequently observed just east of the center of the substorm current system, not at its center. Furthermore, magnetic reconnection is preferentially observed only in the 2-h MLT range (39 out of 56 events). It is important to account for the ambiguity in determining the center of the substorm current system. The average separation between the station with positive D deflection and that with negative D

deflection is 1.7-h, so that it is highly likely that the estimated center positions are scattered. The MLT extent of magnetic reconnection is likely further confined and is estimated to be 1-h in MLT.

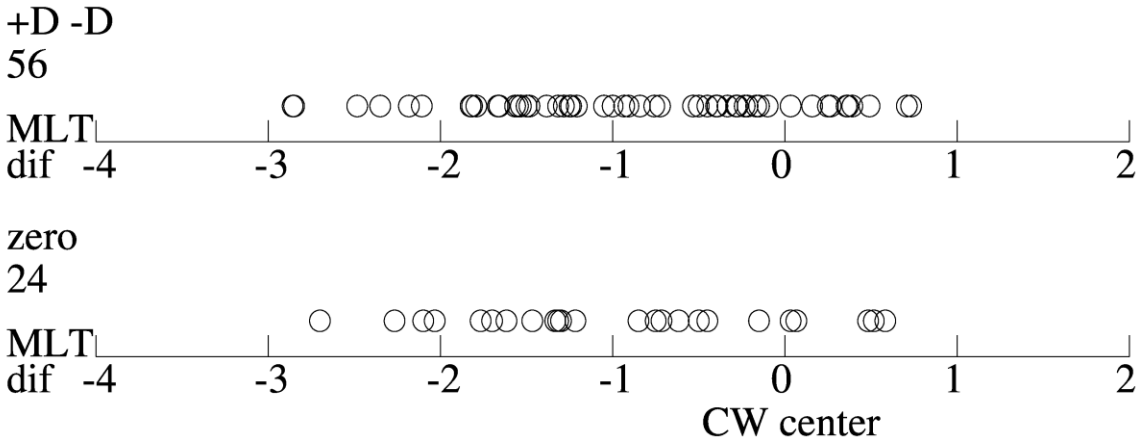

Figure 15. MLT location of the magnetic reconnection site relative to the center of the substorm current wedge. The center of the current wedge is determined using positions with positive and negative D variations (upper panel) and with zero D variation (lower panel).

4.2 Dipolarization at geosynchronous altitude

The GOES spacecraft observations have limitation. High time resolution (0.512-s) magnetic field and electron and proton observations are only available for the events after 2015. It is necessary to use 1-min average magnetic field data for the events in the period of 1994–2014. Unfortunately, we only have a small number of events (6 events with high time resolution data and 12 events with 1-min data) and there were no good Geotail-GOES conjunctions. We classified the variations at geosynchronous altitude into four types: rapid dipolarization with positive D deflection, rapid dipolarization with negative D deflection, slow dipolarization, and no variation. Nagai et al. (2019) compiled the average variations in the magnetic field for dipolarization associated with proton and electron injections at geosynchronous altitude. Rapid dipolarization occurs within 4 min and the change in the H component is more than 10 nT: see Figures 11 and 12 of Nagai et al. (2019). Here, we adopt the criterion that the H component of the magnetic field changes more than 10 nT for the 5-min period for rapid dipolarization with the 1-min data. In most cases, there is a pair of GOES spacecraft (at 75° W and 135° W) available. The data point from GOES-7 at 112° W for the 22 November 1994 event is plotted as a dipolarization with a positive D deflection because the ground D deflection is positive at BOU at 125° W. Figure 16 shows substorm signatures at geosynchronous altitude relative to the Geotail meridian in MLT. A rapid dipolarization with a positive D deflection occurs near the Geotail footpoint meridian, while a rapid dipolarization with a negative D deflection occurs east of the Geotail meridian. Slow dipolarization is observed far from the Geotail meridian. In MLTs very far from the Geotail meridian, no variation is detected at geosynchronous altitude. The local time

extent of the rapid dipolarization is consistent with previous statistical studies with medium time resolution (less than 3 s) magnetic field data (e.g., Nagai, 1982, 1987, 1991).

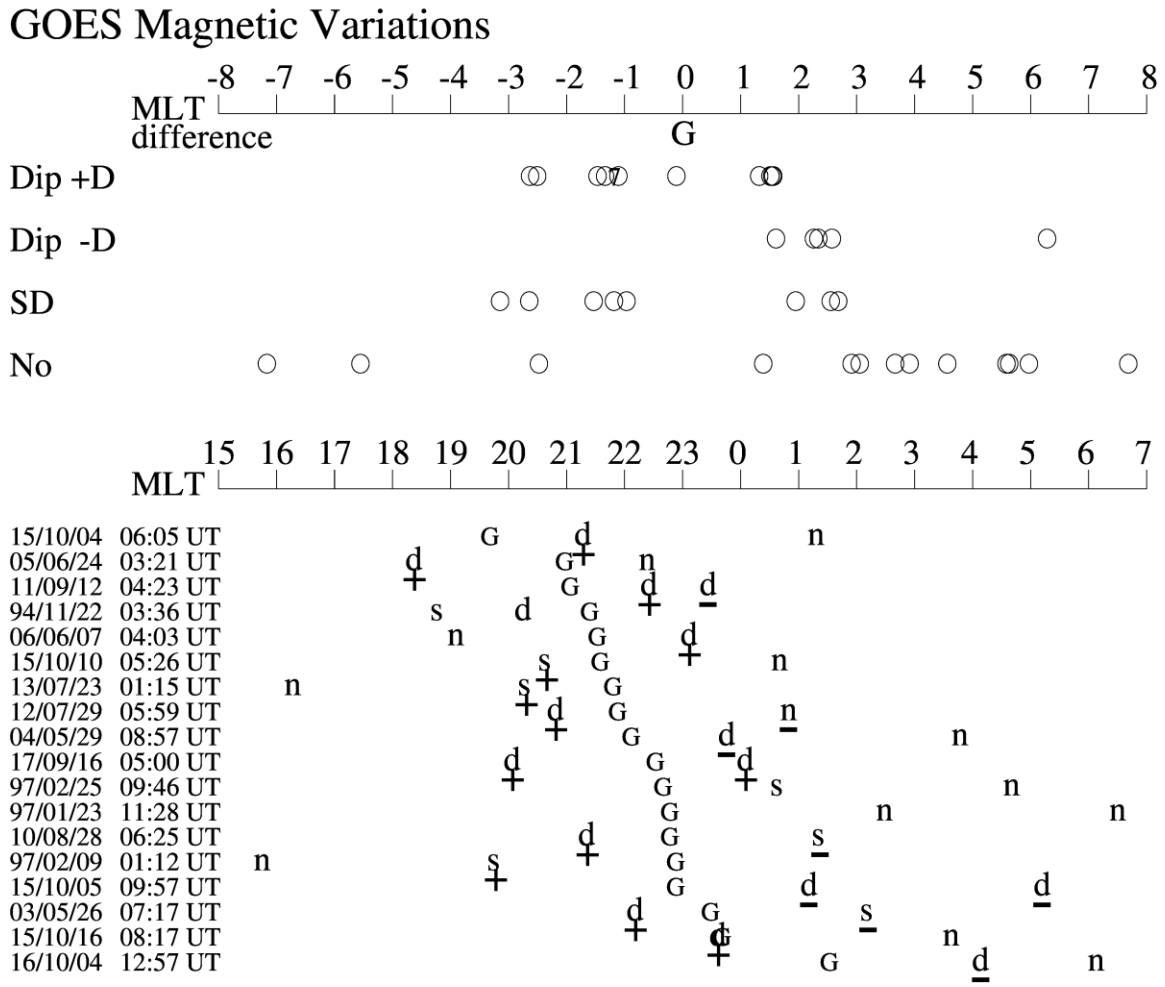

Figure 16. Magnetic field variations at geosynchronous altitude relative to the magnetic reconnection site meridian. The upper panel shows a summary for four classes (rapid dipolarization with positive D deflection, rapid dipolarization with negative D deflection, slow dipolarization, and no variation) and the lower panel shows variations for individual events. ”d” indicates dipolarization, and ”s” indicates slow dipolarization. The D deflection sign is also indicated. ”no” indicates no changes.

5 Discussion

The findings in Sections 3 and 4 can be summarized as follows.

(1) Magnetic reconnection is observed in the upward field-aligned current region of the substorm current system.

(2) The dawn–dusk extent of the magnetic reconnection site is limited to the 1-h local time sector of the upward field-aligned current region, which is located just west of the center of the substorm current system.

493 (3) There are no examples in which magnetic reconnection proceeds in the downward field-
494 aligned current region of the substorm current system.
495 (4) When magnetic reconnection occurs in the far-dusk magnetotail, the center of the substorm
496 current system forms in the far-dusk sector.
497 (5) When magnetic reconnection occurs in the dawn magnetotail, the center of the substorm
498 current system forms in the dawn sector.
499 (6) Rapid dipolarization occurs with a positive D perturbation in the magnetic field at
500 geosynchronous altitude in the meridian of the magnetic reconnection site.
501
502 It is important to note that there is some ambiguity in linking of the magnetic
503 reconnection site to other magnetospheric and ionospheric processes. The calculation of the
504 Geotail footpoint depends on the magnetic field model for the field line tracing. Hall magnetic
505 fields are created near the magnetic reconnection site (e.g., Sonnerup, 1979; Nagai et al., 2001).
506 Positive By deflection is induced in the field lines in the Northern Hemisphere earthward of the
507 magnetic reconnection site, while negative By deflection is induced in the field lines in the
508 Southern Hemisphere. The Hall physics may not be included in the magnetic field model;
509 however, the By bending induced by Hall physics appears to be local in nature (Nagai et al.,
510 2011; 2013a; 2013b; 2015a). It is likely that there are no large systematic errors in determining
511 the footpoint MLT. It is difficult to quantitatively evaluate the ground magnetic field variations
512 over a wide area using the limited number of available stations. For most events, we had five
513 ground stations. We used the events in which a ground station was available near the Geotail
514 footpoint. Ground magnetic field variations include effects from various current systems
515 including previously occurring substorm activities. We can identify a newly formed positive bay
516 signatures for each event. In our analyses, we checked the solar wind conditions, especially the
517 dynamic pressure changes, using the OMNI data. Any changes in the solar wind were excluded
518 from these analyses. Even though there might be other factors affecting our analyses, the results
519 derived in this study are robust and consistent.
520
521 Note that the D deflection signatures at geosynchronous altitude can be different from
522 those on the ground near the center of the substorm current system. A D deflection is always
523 accompanied by dipolarization in the field in all MLT regions (Nagai, 1982, 1991). The D
524 defection signs are the same in both the morning and evening sectors. However, irregular
525 disturbances in D can be found at geosynchronous altitude in the pre-midnight sector (Nagai,
526 1987). Conversely, the D deflection is rather smooth on the ground and, occasionally, no D
527 defection is detected near the center of the substorm current system where the magnitude of a
528 positive bay has its maximum (see, for example, the 4 October 2015 and 4 October 2016 events).
529 This is easily understandable. The ground variations are produced by an integrated effect of the
530 large-scale current system, while the variations at geosynchronous altitude are largely
531 determined by nearby local currents, as suggested by the simple model (e.g., Nagai, 1987). These
532 previous results are based on analyses using 3 s GOES magnetic field data. A recent study using
533 the high time-resolution (0.512 s) magnetic field data with simultaneous proton and electron
534 observations shows much more spikey positive D variations in association with proton injections
535 at geosynchronous altitude, and intense dipolarization in the field takes place with proton
536 injection just west of the D sign change, rather than at the D sign change meridian (Nagai et al.,
537 2019). A positive D spike indicating an upward field-aligned current can be detected at the
538 meridian where the ground D deflection is nearly zero (Nagai et al., 2019). Unfortunately, the

GOES magnetic field data can be examined only for a limited number of events (18 events) and the high time resolution data are even further limited (6 events). The finding of the statistical study is straightforward: a rapid dipolarization with a positive D spike forms in the magnetic field at geosynchronous altitude near the magnetic reconnection site meridian.

One might expect there to be a lot of conjunctions between Geotail and the various spacecraft. MMS was located in the inner magnetosphere (at radial distances of 7.6–8.4 R_E) near the Geotail meridian for the 16 September 2017 event (Section 3.1). MMS Plasma observations were turned off during this event. MMS observed dipolarization around 0500 UT near the 2150 MLT meridian and almost no variations (only a slight increase in Bz) in the magnetic field for the 0430 UT substorm near the 21:35 MLT meridian. The observations provided by MMS confirm the results from the Geotail-GOES pairs but do not add any further information. We did not find any good conjunctions of Geotail with Cluster or THEMIS. The direct causality of magnetic reconnection in the mid-tail with respect to dipolarization in the inner magnetosphere will be strengthened with increased numbers of events observed by future multipoint missions.

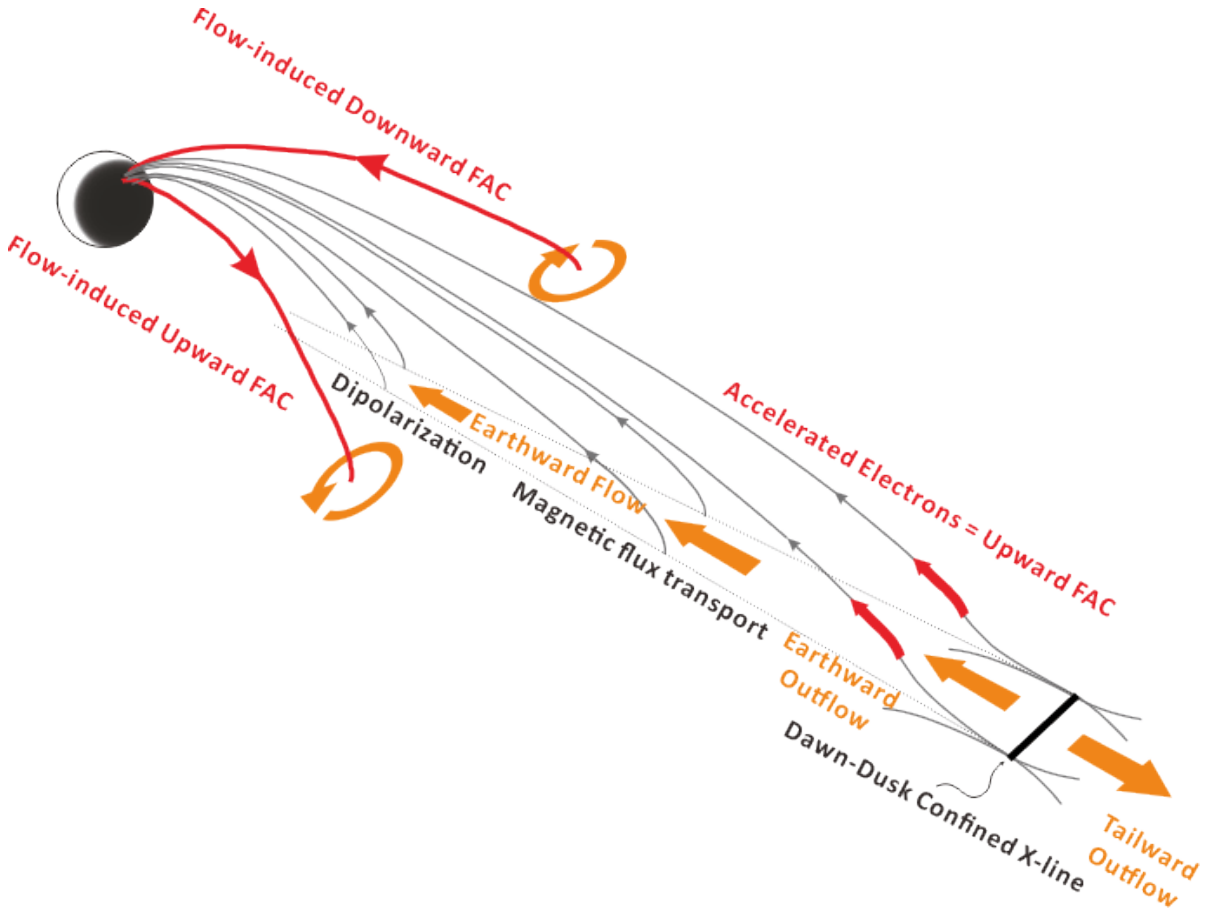

Figure 17. Schematic of the magnetotail dynamics for the expansion phase of a substorm. Magnetic reconnection forms with a dawn–dusk width of approximately 4 R_E beyond X_{GSM} = −20 R_E. Black curves present the magnetic field lines. Field-aligned currents carried by accelerated electrons flow only when the field lines are connected with the magnetic reconnection site. The field lines are transported with earthward flows, resulting in dipolarization in the inner magnetosphere.

The presented study helps refine our understating of the roles of earthward outflows from magnetic reconnection in substorm dynamics. Figure 17 shows a schematic of the substorm dynamics derived from the presented results and previous studies; this is a modification of the schematic presented by Fairfield et al. (1999). In Figure 17, the time evolution of the reconnected field lines is schematically illustrated. Magnetic reconnection forms on the X-line beyond $X_{GSM} = -20\ R_E$ for a limited dawn–dusk length. The high occurrence of magnetic reconnection in the MLT range (Figure 15) suggests the length of 4 R_E in the dawn-dusk direction at a radial distance of 25 R_E if we adopt the Tsyganenko TA15 magnetic field model (Tsyganenko & Andreeva, 2015). The short dawn-dusk length of the X-line implies that magnetic reconnection has the two-dimensional structure in the magnetotail and that any three-dimensional effects might not arose for magnetic reconnection in the near-Earth magnetotail. Indeed, the structure of magnetic reconnection in the near-Earth magnetotail is fully consistent with a picture from two-dimensional full-particle simulations (e.g., Nagai et al., 2011; Zenitani & Nagai, 2016).

Accelerated electrons in the magnetic reconnection site can become field-aligned outflows near the separatrix (e.g., Nagai et al., 1998, 2001). Because the electron flow speed significantly exceeds the ion flow speed, these electron outflows can become upward (from the ionosphere to the tail) field-aligned currents. The Hall electrons flowing into the magnetic reconnection site co-exist in the outer part of the separatrix layer and form the bi-directional electron distributions (e.g., Nagai et al., 1998, 2001). The Hall electrons can form downward (from the tail into the ionosphere) field-aligned currents. The current structure in the vicinity of the magnetic reconnection site is presented in Nagai et al. (2003). The double-current sheet structure is a natural consequence of magnetic reconnection and should be confined to a limited sector. Indeed, a double-current sheet structure is observed in the pre-midnight sector in the vicinity of the geosynchronous altitude (Nagai et al., 1987).

The earthward outflow from the magnetic reconnection near the equatorial plane immediately transforms into MHD flows (Nagai et al., 2011, 2013b) in a spatially limited flow channel carrying magnetic flux, and likely results in dipolarization in the magnetic field in the inner magnetosphere. It is well established that dipolarization starts in a limited (likely less than 1-h) local time sector in the pre-midnight region at geosynchronous altitude (e.g., Nagai, 1982, 1987). Furthermore, it is known that intense upward field-aligned currents exist in the confined region in association with a westward traveling surge on the evening side and that the downward field-aligned current layer exists north of the intense upward field-aligned currents. This is demonstrated by the modeling from ground magnetic field observations by Inhester et al. (1981) and the direct low-altitude satellite Dynamics Explorer observations by Hoffman et al. (1994). The electric field is southward there in the Northern Hemisphere, such that the electric field direction is consistent with the negative Hall electric field ($E_z < 0$ above the neutral sheet and $E_z > 0$ below the neutral sheet) in the ion-electron decoupling region of magnetic reconnection. It is expected that the current system in the vicinity of the magnetic reconnection site is connected to the current system just above the ionosphere.

Generation mechanisms of the substorm current system, which can be simplified as a substorm current wedge, have been proposed, staring with the pioneering study by Vasyliunas (1970). A comprehensive review of current knowledge is given by Kepko et al. (2015). An

intense and narrow earthward flow induces vortex-like motions and pressure changes on both sides. It is possible that downward field-aligned currents on the morning side and upward field-aligned currents on the evening side can be produced by this mechanism and the current wedge can be modeled using computer simulations (e.g., Birn and Hesse, 1991). Recently, Chu et al. (2021) provided an event study supporting this scenario, even though an in situ observation of magnetic reconnection was not identified during their event. Their study suggests that the field-aligned currents contributing to the ground magnetic field variations are generated in the much more near-Earth magnetotail (inside 15 R_E), where the earthward flow makes dawnward and duskward diversions. This is highly possible because flow diversions can be found near a radial distance of 10 R_E in the magnetotail in spacecraft observations (e.g., Nagai et al., 2000) and the dipolarization sector expands dawnward and duskward at geosynchronous altitude (e.g., Nagai, 1982). However, this generation mechanism cannot produce any intense currents in the flow channel itself. The field-aligned current signatures are always observed with dipolarization and the most intense signatures appear for upward field-aligned currents at geosynchronous altitude (Nagai et al., 2019).

There is a possibility that the field-aligned current signatures at geosynchronous altitude can be classified into three types. Nagai et al. (2019) compiled the average D variations constructed via superposed epoch analyses using three simultaneous spacecraft observations at geosynchronous altitude. The timing of the proton injection and the rapid electron flux increase is used as the zero epoch (it is difficult to discriminate injection from flux recovery due to the adiabatic process in the electron flux data). The positive D variations are sharp and spiky at positions where proton injection occurs simultaneously. This behavior is primarily observed in the pre-midnight region. The positive D variations in the early evening sector are more gradual. The negative D variations are always long-lived even when electron injections are simultaneously observed, and the negative D perturbations become much more gradual in the morning sector. The gradual positive D variations in the early evening region and the gradual negative D variations, as well as all D variations on the ground can be attributed to the effect of the vortex-induced and pressure-change-induced field-aligned currents. Spiky positive D variations are likely caused by localized upward field-aligned currents connected with the magnetic reconnection site. The effect of the localized upward field-aligned currents might be minimized with the integration effect of the large-scale current system. The complex D variations at the pre-midnight geosynchronous altitude can be attributed to the double-current structure connected with the magnetic reconnection site. Comparisons of the D signatures at geosynchronous altitude and those on the ground need to be further investigated.

6 Conclusions

In this study, ground magnetic field and geosynchronous substorm signatures were examined for magnetic reconnection events observed in the near-Earth magnetotail. The principal finding, which might be somewhat unexpected, is that in situ magnetic reconnection observations in the near-Earth magnetotail are only found in the upward field-aligned current regions of the substorm current system. Furthermore, magnetic reconnection occurs on the X-line with the 1-hr dawn–dusk length, which is located just west of the center of the substorm current system. The short X-line length implies that magnetic reconnection for substorm onsets is two-

dimensional in nature. Magnetic reconnection in the far-dusk and far-dawn sectors is associated with a newly formed substorm current system in the same local time sector; therefore, there is no dawnward or duskward extension of the X-line for magnetic reconnection in the near-Earth magnetotail. The presented study refines our understanding of substorm dynamics. It is likely that an intense and localized upward field-aligned current is directly connected with the current system formed in the magnetic reconnection site in the near-Earth magnetotail. An intense dipolarization in the inner magnetosphere is produced with earthward outflows from the magnetic reconnection site. Even though the vortex motions and plasma pressure changes in the plasma sheet induced by the earthward outflows are thought to be candidates for the whole substorm current system, their contribution is likely confined to the downward field-aligned currents in the morning sector and the upward field-aligned currents in the early evening sector. Geotail has had a number of encounters with magnetic reconnection in the near-Earth magnetotail during its long observation period; however, good conjunctions with other spacecraft are limited. It is desirable to confirm the presented results with various multipoint observations in space. Furthermore, a formation mechanism for the limited dawn–dusk length X-line in the near-Earth magnetotail needs to be explored.

Acknowledgments

TN thanks D. H. Fairfield for informative discussion. The work of TN at ISAS/JAXA was supported by MEXT/JSPS KAKENHI grant 17H06140. All Geotail data are from the Data Archives and Transmission System (DARTS) of the Institute of Space and Astronautical Science (ISAS) (http://www.darts.isas.jaxa.jp) and they are easily obtained. The LEP energy-time spectrograms are presented at http://www.stp.isas.jaxa.jp/geotail/QL/index.html. We calculated the Geotail footpoint using https://sscweb.gsfc.nasa.gov/cgi-bin/Locator.cgi. The GOES data are obtained from NOAA National Centers for Environmental Information (http://www.ngdc.noaa.gov/stp/satellite/goes/index.html) and the NASA/CDAWeb (http://cdaweb.gsfc.nasa.gov). The NASA OMNI data and MMS data are obtained from the NASA/CDAWeb (http://cdaweb.gsfc.nasa.gov). The digital ground magnetic field data and geomagnetic indices are provided by the World Data Center for Geomagnetism at Kyoto University (http://wdc.kugi.kyoto-u.ac.jp/index.html). Information on the ground magnetic stations can be found in Data Catalogue (pdf) of WDC at Kyoto. Some of digital magnetic field data are provided by the THEMIS web site (http://themis.ssl.berkeley.edu/index.shtml). We also used the data from Super MAG (http://supermag.jhuapl.edu/).

References

Baumjohann, W., Pellinen, R. J., Opgenoorth, H. J., & Nielsen, E. (1981). Two dimensional observations of ground magnetic and ionospheric electric field associated with auroral zone currents: Current systems associated with local auroral break-ups, Planet. Space Sci., 29 (4), 431–447.

Birn, J., & Hesse, M. (1991). The substorm current wedge and field-aligned currents in MHD simulations of magnetotail reconnection. *Journal of Geophysical Research, 96(A2)*, 1611–1618. https://doi.org/10.1029/90JA01762

Chu, X., McPherron, R., Hsu, T.-S., Angelopoulos, V., Weygand, J. M., Liu, J., & Bortnik, J. (2021). Magnetotail flux accumulation leads to substorm current wedge formation: A case study.

Journal of Geophysical Research: Space Physics, *126*, 2020JA028342. https://doi.org/10.1029/2020JA028342

Clauer, C. R., & McPherron, R. L. (1974). Mapping of the local time-universal time developing of magnetospheric substorms using mid-latitude magnetic observations, J. Geophys. Res., 79(19), 2811–2820.

Eastwood, J. P., Phan, T.D., Øieroset, M., & Shay, M. A. (2010). Average properties of the magnetic reconnection ion diffusion region in the Earth's magnetotail: 2001–2005 Cluster observations and comparison with simulations, *J. Geophys. Res.*, *115*, A08215, doi:10.1029/2009JA014962

Fairfield, D. H., Mukai, T., Brittnacher, M., Reeves, G. D., Kokubun, S., Parks, G. K., Nagai, T., Matsumoto, H., Hashimoto, K., Gurnett, D. A., & Yamamoto, T. (1999). Earthward flow bursts in the inner magnetotail and their relation to auroral brightenings, AKR intensifications, geosynchronous particle injections and magnetic activity, *J. Geophys. Res.*, *104*, 355-370.

Genestreti, K. J., Fuselier, S. A., Goldstein, J., & Nagai, T. (2013). An empirical model for the location and occurrence rate of near-Earth magnetotail reconnection, *J. Geophys. Res.*, *118*, 6389-6396, DOI: 10.1002/2013JA019125.

Genestreti, K. J., Fuselier, S. A., Goldstein, J., Nagai, T., & Eastwood, J. P. (2014). The location and rate of occurrence of near-Earth magnetotail reconnection as observed by Cluster and Geotail, *Journal of Atmospheric and Solar-Terrestrial Physics*, *121*, 98-109, doi:10.1016/j.jastp.2014.10.005.

Hoffman, R. A., Fujii, R., & Sugiura, M. (1994). Characteristics of the field-aligned current system in the nighttime sector during auroral substorms, *J. Geophys. Res.*, *99*(A11), 21303–21325. doi:10.1029/94JA01659.

Hones, E. W., & Schindler, K. (1979). Magnetotail plasma flow during substorms: A survey with Imp 6 and Imp 8 satellites, *J. Geophys. Res.*, *84*(A12), 7155–7169. doi:10.1029/JA084iA12p07155

Huba, J. D., & Rudakov, L. I. (2002). Three-dimensional Hall magnetic reconnection, *Phys. Plasmas*, *9*, 4435–4438. doi:10.1063/1.1514970.

Imber, S. M., Slavin, J. A., Auster, H. U., & Angelopoulos, V. (2011). A THEMIS survey of flux ropes and traveling compression regions: Location of the near-Earth reconnection site during solar minimum, *J. Geophys. Res.*, *116*, A02201. doi:10.1029/2010JA016026.

Inhester, B., Baumjohann, W., Greewald, R. A., & Nielsen, E. (1981). Joint two-dimensional observations of ground and ionospheric electric fields associated with auroral zone currents, *J. Geophys.*, *49*, 155–162.

Kepko, L., McPherron, R. L., Amm, O., Apatenkov, S., Baumjohann, W., Birn, J., Lester, M, Nakamura, R., Pulkkinen, T. I., & Sergeev, V. (2014). Substorm current wedge revisited. *Space Science Reviews*, *190*(1–4), 1–46. https://doi.org/10.1007/s11214-014-0124-9

Kokubun, S., Yamamoto, T., Acuña, M. H., Hayashi, K., Shiokawa, K., & Kawano, H. (1994). The Geotail magnetic field experiment, *J. Geomagn. Geoelectr.*, *46*, 7-21.

McPherron, R. L., Russell, C. T., & Aubry, M. P. (1973). Satellite studies of magnetospheric substorms on August 15, 1968: 9. Phenomenological model for substorms, *J. Geophys. Res.*, *78*(16), 3131–3149. doi:10.1029/JA078i016p03131.

Mukai, T., Machida, S., Saito, Y., Hirahara, M., Terasawa, T., Kaya, N., Obara, T., Ejiri, M., & Nishida, A. (1994). The low energy particle (LEP) experiment onboard the Geotail satellite, *J. Geomagn. Geoelectr.*, *46*, 669–692.

Nagai, T. (1982). Observed magnetic substorm signatures at synchronous altitude, J. Geophys. Res., 87(A6), 4405–4417. doi:10.1029/JA087iA06p04405.

Nagai, T. (1987). Field-aligned currents associated with substorms in the vicinity of synchronous orbit: 2. GOES 2 and GOES 3 observations, *J. Geophys. Res.*, *92*(A3), 2432–2446. doi:10.1029/JA092iA03p02432.

Nagai, T. (1991). An empirical model of substorm-related magnetic field variations at synchronous orbit, in *Magnetospheric Substorms*, edited Kan, J. R., Potemra, T. A., Kokubun, S., & Iijima, T., pp. 91-95, AGU, Washington, DC.

Nagai, T. (2021). Magnetic reconnection in the near-Earth magnetotail, *Space Physics and Aeronomy Collection Volume 2: Magnetospheres in the Solar System*, Geophysical Monograph 259. Edited by Romain Maggiolo, Nicolas André, Hiroshi Hasegawa, and Daniel T. Welling. American Geophysical Union. John Wiley & Sons, Inc. DOI: 10.1002/9781119815624.ch4.

Nagai, T., Singer, H. J., Ledley, B. G., & Olsen, R. C. (1987). Field-aligned currents associated with substorms in the vicinity of synchronous orbit: 1. The July 5, 1979, substorm observed by SCATHA, GOES 3, and GOES 2, *J. Geophys. Res.*, *92*(A3), 2425–2431. doi:10.1029/JA092iA03p02425

Nagai, T., Mukai, T., Yamamoto, T., Nishida, A., Kokubun, S., & Lepping, R. P. (1997). Plasma sheet pressure changes during the substorm growth phase, *Geophys. Res. Lett.*, *24* (8) 963-966.

Nagai, T., Fujimoto, M., Saito, Y., Machida, S., Terasawa, T., Nakamura, R., Yamamoto, T., Mukai, T., Nishida, A., & Kokubun, S. (1998). Structure and dynamics of magnetic reconnection for substorm onsets with Geotail observations, *J. Geophys. Res.*, *103*, (3), 4419–4440. doi:10.1029/97JA02190.

Nagai, T. & Machida, S. (1998). Magnetic reconnection in the near-Earth magnetotail, in *New Perspectives on the Earth's Magnetotail*, Geophys. Monogr. Ser. 105, pp. 211-224, edited by Nishida, A., Baker, D. N., and Cowley, S. H. W., AGU, Washington, DC.

Nagai, T., Singer, H. J., Mukai, T., Yamamoto, T., & Kokubun, S. (2000). Development of substorms in the near-Earth tail, *Advances in Space Physics*, *25*, 1651-1662.

Nagai, T., Shinohara, I., Fujimoto, M., Hoshino, M., Saito, Y., Machida, S., & Mukai, T. (2001). Geotail observations of the Hall current system: Evidence of magnetic reconnection in the magnetotail, *J. Geophys. Res.*, *106*(A11), 25929–25949. doi:10.1029/2001JA900038.

Nagai, T., Shinohara, I., Fujimoto, M., Machida, S., Nakamura, R., Saito, Y., and Mukai, T. (2003). Structure of the Hall current system in the vicinity of the magnetic reconnection site, *J. Geophys. Res.*, *108*(A10), 1357. doi:10.1029/2003JA009900.

Nagai, T., Shinohara, I., Fujimoto, M., Matsuoka, A., Saito, Y., & Mukai, T. (2011). Construction of magnetic reconnection in the near-Earth magnetotail with Geotail, *J. Geophys. Res.*, *116*, A04222. doi:10.1029/2010JA016283.

Nagai, T., Shinohara, I., Zenitani, S., Nakamura, R., Nakamura, T. K. M., Fujimoto, M., Saito, Y., & Mukai, T. (2013a). Three-dimensional structure of magnetic reconnection in the magnetotail from Geotail observations, *J. Geophys. Res.*, *118*, 1667–1678. doi:10.1002/jgra.50247.

Nagai, T., Zenitani, S., Shinohara, I., Nakamura, R., Fujimoto, M., Saito, Y., & Mukai, T. (2013b). Ion and electron dynamics in the ion-electron decoupling region of magnetic reconnection with Geotail observations, *Journal of Geophysical Research: Space Physics*, *118*, 7703–7713. doi:10.1002/2013JA019135.

Nagai, T., Shinohara, I., & Zenitani, S. (2015a). Ion acceleration processes in magnetic reconnection: Geotail observations in the magnetotail. *Journal of Geophysical Research: Space Physics, 120,* 1766–1783. doi:10.1002/2014JA020737.

Nagai, T., Shinohara, I., & Zenitani, S. (2015b). The dawn-dusk length of the X line in the near-Earth magnetotail: Geotail survey in 1994–2014, *Journal of Geophysical Research: Space Physics, 120,* 8762–8773. doi:10.1002/2015JA021606.

Nagai, T., Shinohara, I., Singer, H. J., Rodriguez, J., & Onsager, T. G. (2019). Proton and electron injection path at geosynchronous altitude. *Journal of Geophysical Research: Space Physics, 124*. https://doi.org/10.1029/2018JA026281.

Nakamura, R., Baumjohann, W., Fujimoto, M., Asano, Y., Runov, A., Owen, C. J., Fazakerley, A. N., Klecker, B., Rème, H., Lucek, E. A., Andre, M., & Khotyaintsev, Y. (2008). Cluster observations of an ion-scale current sheet in the magnetotail under the presence of a guide field, *J. Geophys. Res., 113,* A07S16, doi:10.1029/2007JA012760.

Nakamura, T. K. M., Nakamura, R., Alexandrova, A., Kubota, Y., & Nagai, T. (2012). Hall magnetohydrodynamic effects for three-dimensional magnetic reconnection with finite width along the direction of the current, *J. Geophys. Res., 117,* A03220. doi:10.1029/2011JA017006.

Oka, M., Phan, T.-D., Øieroset, M., & Angelopoulos, V. (2016). In situ evidence of electron energization in the electron diffusion region of magnetotail reconnection, *J. Geophys. Res. Space Physics, 121,* 1955–1968, doi:10.1002/2015JA022040.

Shay, M. A., Drake, J. F., Swisdak, M., Dorland, W., & Rogers, B. N. (2003). Inherently three dimensional magnetic reconnection: A mechanism for bursty bulk flows?, *Geophys. Res. Lett., 30*(6), 1345. doi:10.1029/2002GL016267.

Shukhtina, M. A., Dmitrieva N. P., & Sergeev, V. A. (2014). On the conditions preceding sudden magnetotail magnetic flux unloading, *Geophys. Res. Lett., 41,* 1093–1099. doi:10.1002/2014GL059290.

Sonnerup, B. U. Ö. (1979), Magnetic field reconnection in *Solar system plasma physics, solar system plasma processes,* Vol. 3, pp. 45-108. Edited by Lanzerotti, L. T., Kennel, C. F., & Parker, E. N. North-Holland, New York.

Torbert, R. B., Burch, J. L., Phan, T. D., Hesse, M., Argall, M. R., Shuster, J., et al. (2018). Electron-scale dynamics of the diffusion region during symmetric magnetic reconnection in space. *Science*. https://doi.org/10.1126/science.aat2998

Tsyganenko, N. A., & Andreeva, V. A. (2015). A forecasting model of the magnetosphere driven by an optimal solar wind coupling function. *Journal of Geophysical Research: Space Physics, 120,* 8401-8425. https://doi.org/10.1002/2015JA021641

Vasyliunas, V. M. (1970), Mathematical models of magnetospheric convection and its coupling to the ionosphere, pp. 60-71, in *Particles and Fields in the Magnetosphere*, Edited by McCormac, B. M. Springer, Dordrecht.

Zenitani, S., & Nagai, T. (2016). Particle dynamics of the electron current layer in collisionless magnetic reconnection, Physics of Plasmas, 23, 102102. http://dx.doi.org/10.1063/1.4963008

Figure Captions

Figure 1. Ground magnetic field data (H and D components) from Fresno (FRN), Tucson (TUC), Boulder (BOU), Stennis (BSL), Fredericksburg (FRD) and San Juan (SJG) for the period of 0400–0600 UT on 16 September 2017. The vertical line on the right side corresponds to 30 nT for FRN, TUC, BOU, BSL, and FRD and 15 nT for SJG.

Figure 2. Magnetic reconnection observations by the spacecraft Geotail for the period of 0400–0600 UT on 16 September 2017. From top to bottom: magnetic field Bx, By, Bz, and Btotal (Bt) [nT], ion flow velocity Vx and Vy [km s^{-1}], number density [cm^{-3}], electron temperature [keV] and electron energy-time spectrogram. Electron counts are presented with a color code (red for high flux and blue for low flux) in the energy (0.1–40 keV)-time spectrogram.

Figure 3. The magnetic field (H, V, D, and Btotal in nT and inclination in degrees) and the 30–50-, 50–100-, 100–200-, 200–350-, and 350–600-keV electron and 80–110-, 110–170-, 170–250-keV proton fluxes for GOES-15 and GOES-13 for the period of 0400–0600 UT on 16 September 2017. The electron and proton fluxes are given in $cm^{-2}\ s^{-1}\ sr^{-1}\ keV^{-1}$.

Figure 4. Summary of the 0505 UT and 0432 UT events on 16 September 2017. The Geotail magnetic local time (MLT) location (represented by G) is shown at 22:34 MLT for the 0505 UT event and at 22:28 MLT for the 0432 UT event. The D deflection at the ground station is indicated by "+" for positive and "-" for negative at its MLT position. The positive D deflection region corresponding to the upward field-aligned current region is indicated by a horizontal line, while the negative D deflection region corresponding to the downward field-aligned current region is indicated by a dashed horizontal line. The rapid dipolarization at geosynchronous altitude is indicated by D with G13 indicating GOES-13 and with G15 indicating GOES-15. N indicates less pronounced dipolarization.

Figure 5. Ground magnetic field data (H and D) from Apia (API), Honolulu (HON), Papeete (PPT), Fresno (FRN), Tucson (TUC), Boulder (BOU), Stennis (BSL), and Fredericksburg (FRD) for the period of 0500–0700 UT on 4 October 2015. The sign of the D component from the Southern Hemisphere stations API and PPT is reversed. The vertical line on the right side corresponds to 20 nT for API, PPT, and HON and 50 nT for the other stations. For D, the vertical line on the right side corresponds to 10 nT for API and PPT.

Figure 6. Magnetic reconnection observations by the spacecraft Geotail for the period of 0500–0700 UT on 4 October 2015. From top to bottom: magnetic field Bx, By, Bz, and Btotal [nT], ion flow velocity Vx and Vy [km s^{-1}], number density [cm^{-3}], electron temperature [keV] and electron energy-time spectrogram.

Figure 7. The magnetic field (H, V, D, and Bt in nT and inclination in degrees) and the 30–50-, 50–100-, 100–200-, 200–350-, and 350–600-keV electron and the 80–110-, 110–170-, 170–250-keV proton fluxes for GOES-15 and GOES-13 for the period of 0500–0700 UT on 4 October 2015. The electron and proton fluxes are given in $cm^{-2}\ s^{-1}\ sr^{-1}\ keV^{-1}$.

Figure 8. Summary of the 0605 UT and 0525 UT events on 4 October 2015, notation as in Figure 4.

Figure 9. Ground magnetic field data (H and D) from Kakioka (KAK), Charters Towers (CTA), Canberra (CNB), Apia (API), Honolulu (HON), Papeete (PPT), and Fresno (FRN) for the period of 1130–1330 UT on 4 October 2016. The sign of the D component from the Southern Hemisphere stations CTA, CNB, API, and PPT is reversed. The vertical line on the right side corresponds to 20 nT for API, HON, and PPT and 30 nT for the other stations. For D, the vertical line on the right side corresponds to 10 nT for API and PPT.

Figure 10. Magnetic reconnection observations by Geotail for the period of 1130–1330 UT on 4 October 2016. From top to bottom: magnetic field Bx, By, Bz, and Btotal [nT], ion flow velocity Vx and Vy [km s^{-1}], number density [cm^{-3}], electron temperature [keV] and electron energy-time spectrogram.

Figure 11. The magnetic field (H, V, D, and Bt in nT and inclination in degrees), the 30–50-, 50–100-, 100–200-, 200–350-, and 350–600-keV electron and, the 80–110-, 110–170-, 170–250-keV proton fluxes for GOES-15 and GOES-13 for the period of 0400–0600 UT on 4 October 2016. The electron and proton fluxes are given in $cm^{-2}\ s^{-1}\ sr^{-1}\ keV^{-1}$.

Figure 12. Summary of the 1257 UT and 1152 UT events on 4 October 2016, notation as in Figure 4.

Figure 13. Location of magnetic reconnection events in the Geotail footpoint MLT versus the geomagnetic latitude diagram (upper panel) and in the GSM x-y plane (lower panel). The three dots indicate the events described in Section 3.

Figure 14. Ground D variations during magnetic reconnection relative to the Geotail footpoint in the MLT diagram. The upper panel shows all the data points (three different classes) from the 56 events, and the lower panel shows the D variations for each event (“+” for positive D, “– “ for negative D, and “o” for no variation).

Figure 15. MLT location of the magnetic reconnection site relative to the center of the substorm current wedge. The center of the current wedge is determined using positions with positive and negative D variations (upper panel) and with zero D variation (lower panel).

Figure 16. Magnetic field variations at geosynchronous altitude relative to the magnetic reconnection site meridian. The upper panel shows a summary for four classes (rapid dipolarization with positive D deflection, rapid dipolarization with negative D deflection, slow dipolarization, and no variation) and the lower panel shows variations for individual events. ”d” indicates dipolarization, and ”s” indicates slow dipolarization. The D deflection sign is also indicated. ”no” indicates no changes.

Figure 17. Schematic of the magnetotail dynamics for the expansion phase of a substorm. Magnetic reconnection forms with a dawn–dusk width of approximately 4 R_E beyond X_{GSM} = −20 R_E. Black curves present the magnetic field lines. Field-aligned currents carried by

914 accelerated electrons flow only when the field lines are connected with the magnetic
915 reconnection site. The field lines are transported with earthward flows, resulting in dipolarization
916 in the inner magnetosphere.